

1 **Mid- to late Holocene morphological and hydrological changes in the south**  
2 **Taihu area of the Yangtze delta plain, China**

3  
4 Ting Chen<sup>a, b</sup>, David B. Ryves<sup>c</sup>, Zhanghua Wang<sup>a\*</sup>, Jonathan P. Lewis<sup>c</sup>, Xuening  
5 Yu<sup>a</sup>  
6

7 <sup>a</sup> *State Key Laboratory of Estuarine and Coastal Research, East China Normal*  
8 *University, Shanghai 200062, China*

9 <sup>b</sup> *Academy for Advanced Interdisciplinary Studies, Southern University of*  
10 *Science and Technology, Shenzhen 518055, China*

11 <sup>c</sup> *Centre for Hydrological and Ecosystem Science, Department of Geography,*  
12 *Loughborough University, Loughborough LE11 3TU, UK*

13  
14 *\*Corresponding author:*

15 *Zhanghua Wang, State Key Laboratory of Estuarine and Coastal Research, East*  
16 *China Normal University, Shanghai 200062, China.*

17 *Tel: +86 13817202106*

18 *E-mail address: zhwang@geo.ecnu.edu.cn*  
19

20 **Abstract**

21 The Taihu Plain of the Lower Yangtze valley, China was a centre of rice  
22 agriculture during the Neolithic period. Reasons for the rapid development of rice  
23 cultivation during this period, however, have not been fully understood for this coastal  
24 lowland, which is highly sensitive to sea-level change. To improve understanding of  
25 the morphological and hydrological context for evolution of prehistoric rice

26 agriculture, two sediment cores (DTX4 and DTX10) in the East Tiaoxi River Plain,  
27 south Taihu Plain, were collected, and analysed for radiocarbon dating, diatoms,  
28 organic carbon and nitrogen stable isotopes ( $\delta^{13}\text{C}$  and  $\delta^{15}\text{N}$ ), grain size and lithology.  
29 These multiproxy analyses revealed that prior to ca. 7500 cal. yr BP, the East Tiaoxi  
30 River Plain was a rapidly aggrading high-salinity estuary (the Palaeo-Taihu Estuary).  
31 After ca. 7500 cal. yr BP, low salinity conditions prevailed as a result of strong  
32 Yangtze freshwater discharge. Subsequently, seawater penetration occurred and  
33 saltmarsh developed between ca. 7000 and 6500 cal. yr BP due to accelerated relative  
34 sea-level rise. This transgression event influenced a large area of the Taihu Plain  
35 during the Holocene, as shown by multiple sediment records from previous studies.  
36 Persistent freshwater marsh (or subaerial land) formed due to dramatic  
37 shrinkage/closure of the Palaeo-Taihu Estuary after ca. 5600 cal. yr BP when sea level  
38 was relatively stable. We speculate that morphological and hydrological changes of  
39 the East Tiaoxi River Plain played an important role in agricultural development  
40 across the Taihu Plain during the Neolithic period. The closure of the Palaeo-Taihu  
41 Estuary and the formation of stable freshwater marsh (or subaerial land) after ca. 5600  
42 cal. yr BP were critical preconditions encouraging the rapid rise of rice productivity in  
43 the Liangzhu period (5500-4500 cal. yr BP). This development changed the landscape  
44 and river systems, and thus provided adequate freshwater supply to the Taihu Plain.

45

#### 46 **Key words**

47 Coastal wetland; Salinity; Sea level; Freshwater resource; Rice agriculture,  
48 Multiproxy analyses

49

#### 50 **1. Introduction**

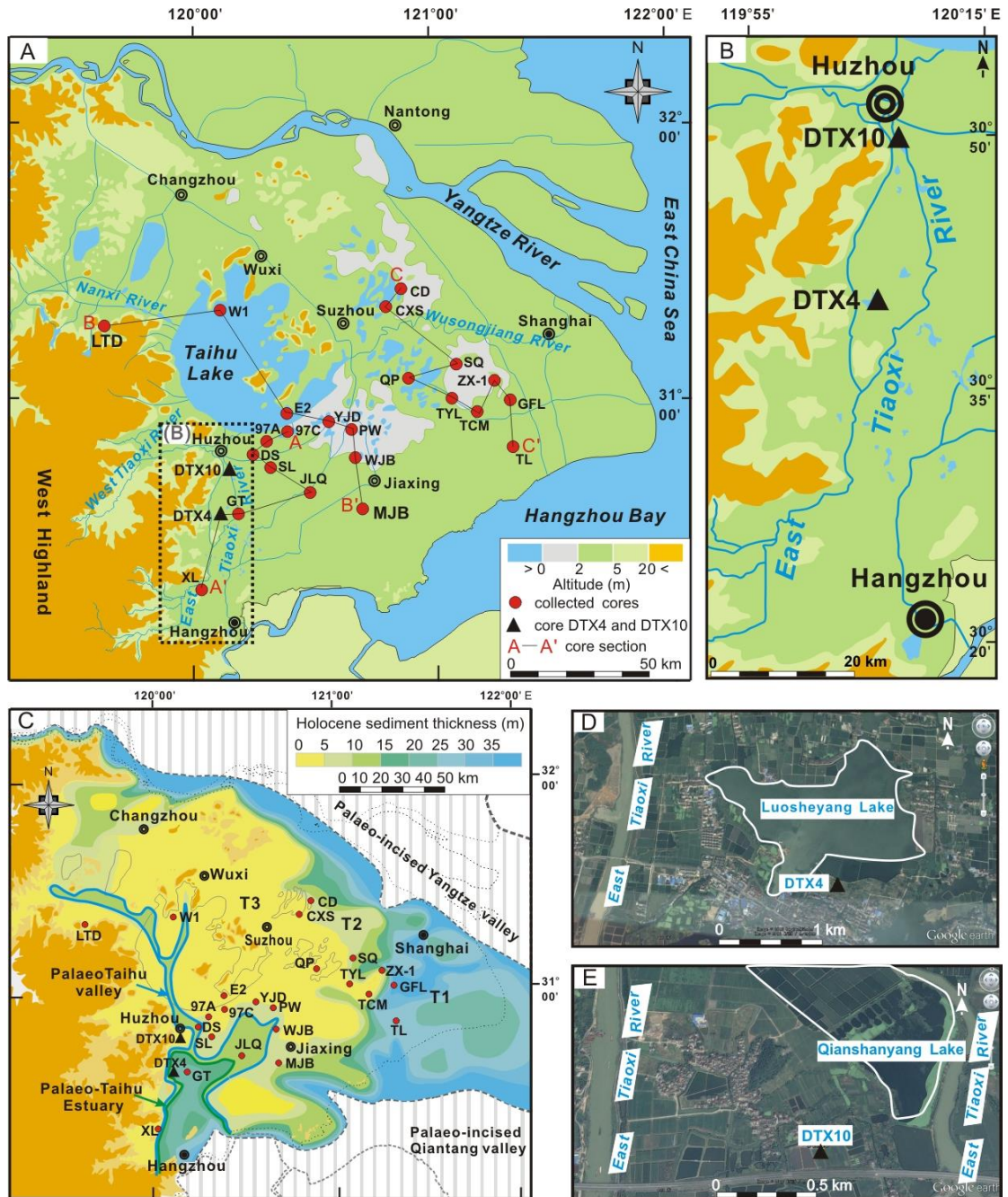
51 The lower Yangtze valley, East China is one of the centres where intense rice  
52 growth started in the Neolithic period (Zong et al., 2007; Liu and Chen, 2012). Many  
53 studies have been focused on the origin and domestication of rice farming in this  
54 region during the Neolithic cultural period (Zong et al., 2007; Mo et al., 2011; Liu and  
55 Chen, 2012). The first evidence of collection and consumption of wild rice (ca.  
56 9000-10000 cal. yr BP) was found at Shangshan site, in Zhejiang Province (Liu and  
57 Chen, 2012; Zuo et al., 2017). Evidence for rice cultivation also found at the  
58 Kuahuqiao site at ca. 7700 cal. yr BP (Zong et al., 2007). Although marine inundation  
59 caused by sea-level rise brought rice cultivation to an end at the Kuahuqiao site at ca.  
60 7500 cal. yr BP (Zong et al., 2007), rice farming subsequently expanded to the south  
61 of the Hangzhou Bay and in the Taihu Plain, north of Hangzhou Bay (Chen et al.,  
62 2008; Zong et al., 2012a; Zheng et al., 2012). Rice domestication started during the  
63 period of the Majiabang culture (7000-5800 cal. yr BP), the first Neolithic culture that  
64 appeared on the Taihu Plain, though this society still relied mostly on hunting, fishing  
65 and gathering (Cao et al., 2006; Fuller et al., 2007; Mo et al., 2011; Zong et al., 2012a;  
66 Xu, 2015). More rice cultivation was practiced during the Songze period (5800-5500  
67 cal. yr BP), but hunting, fishing and gathering were still important at that time (Cao et  
68 al., 2006; Mo et al., 2011). Subsequently, rice farming intensified and its yield  
69 increased dramatically during the Liangzhu culture (5500-4500 cal. yr BP) (Fan, 2011;  
70 Mo et al., 2011; Zhuang et al., 2014; Zhang et al., 2015). For example, substantial  
71 quantities of carbonised rice were found at several Liangzhu sites (Fan, 2011), one of  
72 which even reached to tens of thousands of kilograms; numerous specialised fine  
73 stone tools used for rice farming, such as ploughs and sickles, were also found (Mo et  
74 al., 2011). Relying on rapid advances in rice farming, the Liangzhu culture developed  
75 into a sophisticated and complex society and was considered as one of the most

76 advanced Neolithic societies in the world (Jiang and Liu, 2006; Zhu, 2006; Lawler,  
77 2009; Mo et al., 2011; Zong et al., 2012a; Zhuang et al., 2014).

78 Several studies suggested that a warm/humid climate promoted the development  
79 of rice farming in the lower Yangtze delta (Yu et al., 2000; Chen et al., 2005; Innes et  
80 al., 2009, 2014; Patalano et al., 2015), together with ancient people's successful water  
81 and landscape management of rice paddies (Zong et al., 2007; Zhuang et al., 2014).  
82 Recently, more attention has been paid to the role of the hydrological environment,  
83 which is the result of a complex of sea-level, climate and geomorphological  
84 conditions (Zong et al., 2007; Qin et al., 2011; Zheng et al., 2012; Long et al. 2014;  
85 Patalano et al., 2015). For example, Zong et al. (2007) found that freshwater low-land  
86 swamps at the Kuahuqiao site were selected by Neolithic people for rice cultivation.  
87 Qin et al. (2011) reported that rice-based agriculture occurred during two intervals of  
88 lower salinity, between ca. 7850-7210 cal. yr BP and ca. 3000-2290 cal. yr BP.  
89 Although these studies of hydrological background based on individual cores  
90 provided insights into our understanding of the development of rice farming in the  
91 lower Yangtze valley, new studies on key sites allowing an integrated analysis of  
92 previous studies are still required to provide a more detailed environmental context on  
93 a regional scale.

94 We focus here on the hydrological changes during the mid- to late-Holocene in  
95 the East Tiaoxi River Plain, part of the southern Taihu Plain (Fig. 1A and 1B). The  
96 East Tiaoxi River Plain is a critical part of the Taihu plain, because it was a  
97 palaeo-incised valley during the Last Glacial Maximum (LGM) and was occupied by  
98 the Palaeo-Taihu Estuary during the early- to mid-Holocene (Fig. 1C; Hong, 1991).  
99 Through this estuary, sea water could have reached the centre of the Taihu Plain, and  
100 freshwater from the west uplands, which flows into the Taihu lake at present, instead  
101 was discharged into Hangzhou Bay (Hong, 1991). Such hydrologic conditions had

102 restricted the freshwater resource for Neolithic people in the Taihu Plain.  
 103 Morphological and hydrological changes within the East Tiaoxi River Plain from the  
 104 Mid-Holocene are therefore potentially critical to understanding the evolution of rice  
 105 farming in the Taihu Plain over the Neolithic period.



106  
 107

108 **Fig. 1** Maps of the Taihu Plain and location of study sites. (A) Map of the present Taihu Plain (after  
109 [Song et al., 2013](#)), showing geomorphology, hydrology and locations of core DTX4 and DTX10, and  
110 cores collected from previous studies (red solid circles; references in [supplementary Table 1](#)). (B) Map  
111 of the East Tiaoxi River Plain, including West and East Tiaoxi River and locations of cores DTX4 and  
112 DTX10. (C) Palaeotopographical map of the Taihu Plain during the Last Glacial Maximum (after [Wang](#)  
113 [et al., 2012](#)), showing the Palaeo-Taihu valley (blue solid line) and Palaeo-Taihu Estuary (green solid  
114 line). (D) and (E) Remote sensing image in 2016, around Luosheyang Lake and Qianshanyang Lake  
115 from Google Earth, showing part of East Tiaoxi River and locations of core DTX4 and DTX10,  
116 respectively.

117

118 A complete understanding of the evolution of morphological and hydrological  
119 environments of the East Tiaoxi River Plain during the mid- to late-Holocene,  
120 however, has been hampered by a lack of high-quality sediment archives with reliable  
121 dating allowing detailed sedimentological analysis. To address this gap and fulfill the  
122 research aim mentioned above, two sediment cores (DTX 4 and DTX10), spanning  
123 the last 7100 and 7600 years respectively, were collected beside the Luosheyang Lake  
124 and the Qianshanyang Lake in the East Tiaoxi River Plain in 2014 ([Fig. 1](#)). Using  
125 these two cores, we studied the past morphological and hydrological environments of  
126 the East Tiaoxi River Plain over the last 7600 years, by using a multi-proxy approach  
127 including lithology, grain size, diatom analysis and organic geochemistry (including  
128 stable isotopes of carbon and nitrogen:  $\delta^{13}\text{C}$ ,  $\delta^{15}\text{N}$ ). Additionally, we compared these  
129 new results with the hydrological environment inferred from other parts of the Taihu  
130 Plain from previously studied cores ([Itzstein-Davey et al., 2007](#); [Atahan et al., 2008](#);  
131 [Zong et al., 2011, 2012b](#); [Wang et al., 2012](#); [Innes et al., 2014](#); [Liu et al., 2015](#)). Based  
132 on these results, we discuss how changing morphological and hydrological conditions

133 in the East Tiaoxi River Plain influenced the expansion of rice cultivation in the Taihu  
134 Plain over the Neolithic period.

135

## 136 **2. Study area and site description**

137 During the LGM, the landscape of the Taihu Plain was characterised by a series  
138 of river terraces (T1, T2 and T3) and incised valleys (Fig. 1C) cutting through these  
139 terraces (Yan and Huang, 1987; Li et al., 2000, 2002; Wang et al., 2012). The terraces  
140 T1, T2 and T3 were regions where the thickness of Holocene sediments were at 20-30  
141 m, 5-15 m, and < 5 m, respectively (Yan and Huang, 1987; Li et al., 2000, 2002;  
142 Wang et al., 2012). The largest two of these palaeo valleys were the Yangtze valley in  
143 the north and the Qiantang valley in the south. The Palaeo-Taihu valley lay along the  
144 western highlands, and freshwater discharge from western mountains flowed through  
145 it southwards into the Palaeo-Qiantang valley (Yan and Huang, 1987; Hong, 1991;  
146 Wang et al., 2012). When sea level rose from -18 m to -4 m between ca. 8600 cal. yr  
147 BP and ca. 7300 cal. yr BP, the south part of the Palaeo-Taihu valley became an  
148 estuary, allowing sea water from Hangzhou Bay to reach the central Taihu Plain  
149 (Hong, 1991; Wang et al., 2012).

150 Present-day geomorphological and hydrological conditions of the Taihu Plain,  
151 however, are dramatically different. Today, the Taihu Plain is characterised by a  
152 saucer-like depression, in the centre of which lies Taihu Lake (Fig. 1A), the third  
153 largest freshwater lake in China. Taihu Lake receives freshwater inflows (e.g. the East  
154 and West Tiaoxi Rivers; Fig. 1A) from the mountainous areas to the west of the Taihu  
155 Plain and provides an important freshwater resource for the human population in the  
156 Taihu Plain.

157 The East Tiaoxi River Plain is the southern part of the Taihu Plain and lies  
158 between Taihu Lake in the north and the Qiantang River/Hangzhou Bay in the south

159 (Fig. 1A and 1B). Relief is slightly higher (2-5 m) in the south and east, and lower (<  
160 2 m) in the depression near Taihu Lake. The East Tiaoxi River, the largest river in the  
161 East Tiaoxi River Plain, flows northward into Taihu Lake after joining with the West  
162 Tiaoxi River in the city of Huzhou.

163 Luosheyang Lake and Qianshanyang Lake are located near the East Tiaoxi River  
164 (Fig. 1B, 1D and 1E), and are about 140 km west of Shanghai. They are both naturally  
165 open, shallow (< 2 m maximum depth) and flat-bottomed freshwater lakes, through  
166 which the East Tiaoxi River and its tributaries flow. Over recent decades, the area of  
167 the Luosheyang Lake has been reduced due to extensive marginal development for  
168 agriculture (e.g. rice paddies) to about 1.56 km<sup>2</sup>, while the Qianshanyang Lake has  
169 been almost completely reclaimed.

170

### 171 **3. Material and methods**

#### 172 *3.1 Coring, sampling, AMS <sup>14</sup>C dating and age-depth model*

173 Both cores DTX4 and DTX10, 5.7 and 4.6 m long respectively, were obtained in  
174 May 2014 using a gouge corer (Eijkelkamp Company, the Netherlands), with a  
175 diameter of 3 cm. Core DTX4 (30°38'16.465" N, 120°05'28.546" E) was collected  
176 from a reclaimed agricultural field which was previously the edge of the Luosheyang  
177 Lake, and core DTX10 from a rice paddy near present Qianshanyang Lake (Fig. 1B,  
178 1D and 1E). Lithology of both cores was examined carefully during the drilling,  
179 including particle composition, structure, colour, and presence of plant macrofossils.  
180 Recent cultural sediments at the top of each core were removed (the uppermost 80 cm  
181 at DTX4 and 20 cm at DTX10). Ten plant macrofossils (excluding root material) and  
182 organic-rich samples from the two cores were dated via AMS <sup>14</sup>C dating by Beta  
183 Analytic, USA (Table 1). All conventional dates were calibrated using the INTCAL 13



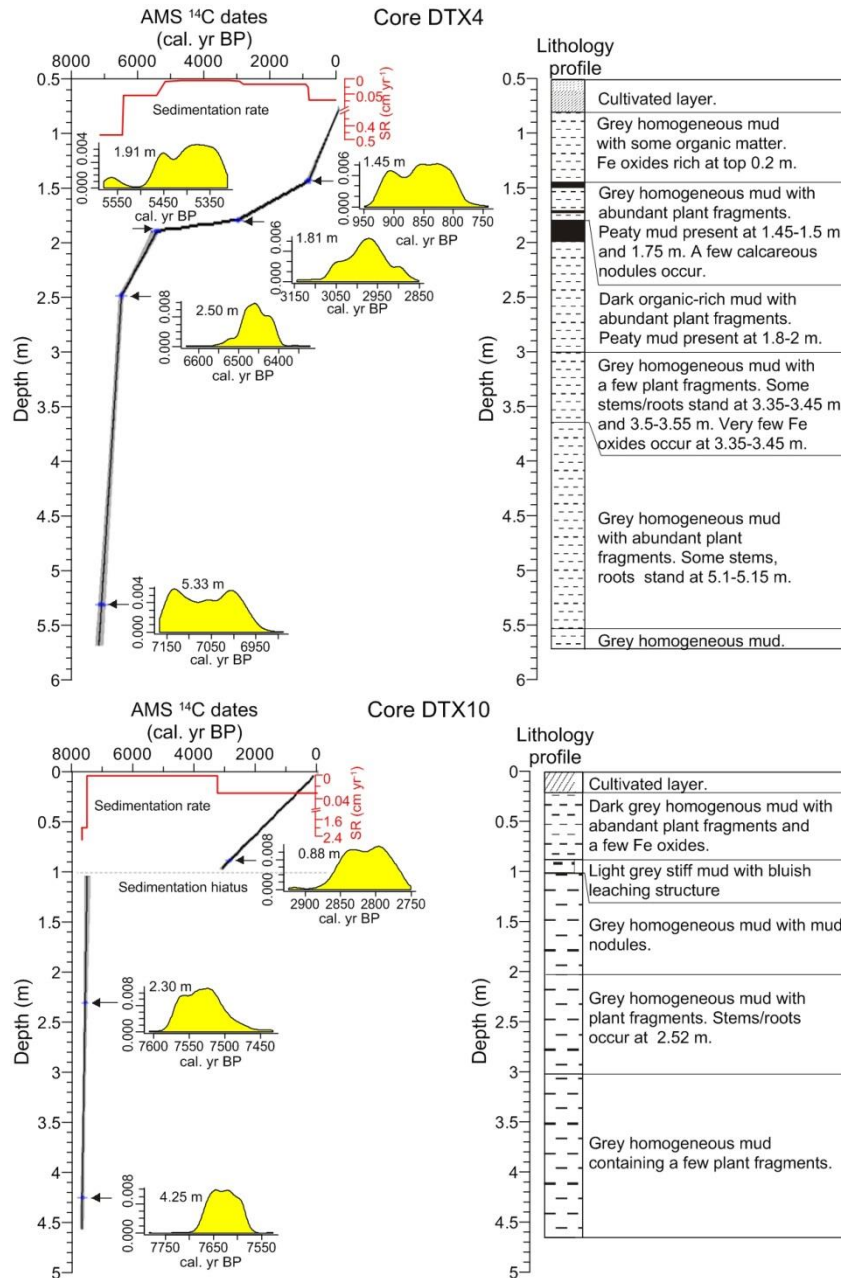
184 database (Talma and Vogel, 1993; Reimer et al., 2009) and calibrated dates with two  
 185 sigma were presented as ‘medial point ages  $\pm$  standard deviation’ (Table 1). A linear  
 186 interpolation method was used to construct the age-depth model, using the program  
 187 ‘Clam’ with 10,000 iterations (Blaauw, 2010; Fig. 2). The sedimentation rate (SR), the  
 188 best estimated age and the minima and maxima of age confidence intervals were  
 189 calculated every 2 cm (core DTX4) and 4 cm (DTX10) simultaneously, using the  
 190 ‘Clam’ program. In addition, , a sedimentation hiatus was identified in core DTX10 at  
 191 a sediment depth of 1.0 m due to a leaching structure indicative of pedogenesis  
 192 (0.88-1.0 m).

193

194 **Table 1** AMS  $^{14}\text{C}$  dating results of core DTX4 and DTX10

195

Core name	Depth (m)	Dated material	$\delta^{13}\text{C}$ (‰)	Conventional age (yr BP)	Calibrated age (2 sigma, cal. yr BP)	Median Calibrated age (cal. yr BP)	Lab. code
<b>Core DTX4</b>	1.21	Plant fragments	-27.2	1610 $\pm$ 30	1560–1410	1485 $\pm$ 75	Beta-383485
	1.45	Plant fragments	-28.8	940 $\pm$ 30	930–785	858 $\pm$ 73	Beta-406458
	1.81	Plant fragments	-27.8	2860 $\pm$ 30	3065–2920	2993 $\pm$ 73	Beta-383486
	1.91	Plant fragments	-26.4	4680 $\pm$ 30	5575–5550	5562 $\pm$ 13	Beta-406459
	2.5	Organic-rich mud	-25.7	5680 $\pm$ 30	6500–6405	6453 $\pm$ 48	Beta-382369
	5.33	Plant fragments	NA	6150 $\pm$ 30	7160–6950	7055 $\pm$ 105	Beta-383487
<b>Core DTX10</b>	0.88	Plant fragments	NA	2720 $\pm$ 30	2870–2760	2815 $\pm$ 55	Beta-382371
	2.3	Plant fragments	-27.6	6650 $\pm$ 30	7580–7480	7530 $\pm$ 50	Beta-382366
	2.91	Organic-rich mud	-25.1	8380 $\pm$ 30	9475–9400	9438 $\pm$ 38	Beta-385582
	4.25	Plant fragments	-26.1	6780 $\pm$ 40	7680–7575	7628 $\pm$ 53	Beta-385583



196

197 **Fig. 2** Age-depth model, sedimentation rate (SR) and density distribution of AMS <sup>14</sup>C dates (shaded in  
 198 yellow) basing on the ‘Clam’ program (Blaauw, 2010), and lithology profile for core DTX4 and  
 199 DTX10. A sedimentation hiatus was identified at 1.0 m in core DTX10 because of clear indications of  
 200 pedogenesis (leaching) apparent in the lithology between 0.88-1.0 m.

201 Sediment subsamples were selected at 2 to 10 cm intervals, using 2 to 5 cm  
202 thick slices, with thickness chosen according to sedimentation rate: in core DTX4,  
203 every 4 cm interval (4 cm thick) from 0.8-1.2 m, 5 cm (5 cm thick) from 1.2-1.8 m, 2  
204 cm (2 cm thick) from 1.8-2.14 m, 3 cm (3 cm thick) from 2.14-2.5 m, and 10 cm (5  
205 cm thick) from 2.5-5.7 m; in core DTX10, every 4 cm (4 cm thick) from 0.2-2.3 m,  
206 and 10 cm (5 cm thick) from 2.3-4.6 m. A total of 84 and 77 subsamples were  
207 obtained for core DTX4 and DTX10 respectively. All subsamples were stored in a  
208 fridge at 4 °C prior to analyses.

### 209 *3.2 Diatom analysis*

210 Diatom concentrations were low in most samples, with a total of only 29 samples  
211 in core DTX4 and 10 in core DTX10 containing diatoms at high enough concentration  
212 to permit using the standard water bath method (Renberg, 1990; Battarbee et al.,  
213 2001). Due to extremely low diatom concentrations, 8 samples in core DTX4 and 19  
214 in core DTX10, were treated with heavy liquid separation (sodium polytungstate, SPT)  
215 using the following procedures (Battarbee and Kneen, 1982; Battarbee et al., 2001).  
216 After organic matter and carbonate were removed using hydrogen peroxide (H<sub>2</sub>O<sub>2</sub>)  
217 and HCl, clay grains were removed by adding a few drops of weak NH<sub>3</sub> solution  
218 (Battarbee et al., 2001). Then, the non-toxic heavy liquid SPT (3Na<sub>2</sub>WO<sub>4</sub>·9WO<sub>3</sub>·H<sub>2</sub>O)  
219 with a density of 2.26 g ml<sup>-1</sup> was used twice to separate diatoms from mineral grains  
220 with a density above this. Diatom slides were made in the regular way using the  
221 diatom-enriched supernatant taken from the top of SPT solutions, after washing with  
222 distilled water. A known number of microspheres were added to all samples to assess  
223 diatom concentration (Battarbee and Kneen, 1982). The average number of diatoms  
224 counted for samples prepared with regular water-bath and SPT method is 266 and 269  
225 valves, respectively, in core DTX4, with the exception of one sample at 5.675 m, for

226 which only 111 valves were counted due to extremely low diatom concentration. The  
227 number of diatoms counted for regularly treated samples was lower in core DTX10  
228 than that in core DTX4 due to lower diatom concentration, but counts of at least 174  
229 valves were obtained with an average of 192, while for SPT treated samples, over 270  
230 valves with an average of 331 were counted. Valves were identified to species level  
231 where possible using general (Krammer and Lange-Bertalot, 1986, 1988, 1991a,  
232 1991b; <http://westerndiatoms.colorado.edu/>) and more specialised coastal floras  
233 (Witkowski et al., 2000). Diatoms were also classified into their salinity (freshwater,  
234 brackish and marine) and habitat preferences (planktonic, benthic), based on the  
235 literature and website resources (e.g. van der Wuff and Huls, 1976; Vos and de Wolf,  
236 1993; Ryves et al., 2004; <http://craticula.ncl.ac.uk/Molten/jsp/>;  
237 <http://www.marinespecies.org/>) and ecological knowledge.

238 In most samples some signs of diatom dissolution were apparent: e.g. thinner  
239 valve walls in the sub-fossil material. Therefore, the state of dissolution for each valve  
240 was recorded and the F-index, the ratio of pristine valves to the sum of pristine and  
241 dissolved valves, was calculated for each sample (Ryves et al., 2001). Even where the  
242 standard water-bath method was suitable, and diatom concentrations were higher  
243 (generally in the fresh water phases), preservation was judged not consistently good  
244 enough to support applying a salinity model (which remain robust; Juggins, 2013), as  
245 poor preservation is known to cause bias in model outputs (e.g. Ryves et al. 2006,  
246 2009). Percentage abundances of diatom data were calculated and plotted using the  
247 stratigraphic software package C2 (Juggins, 1991-2009). Diatom zones were  
248 determined based on cluster analysis using the CONISS function in the programme  
249 Tilia 2.0.41.

### 250 3.3 Grain size analysis

251 Grain size analyses were conducted on each subsample. These samples were  
252 firstly pretreated with 10 % H<sub>2</sub>O<sub>2</sub> and then 10 % HCl to remove organic matter and  
253 carbonates respectively, and then washed in distilled water to remove residual HCl.  
254 Following this, 5 ml of 5 % Calgon® (sodium hexametaphosphate) was added to each  
255 sample before shaking in an ultrasonic bath for 15 minutes to prevent flocculation of  
256 fine-grained particles (Beuselinck et al., 1998). Measurements were performed with a  
257 Beckman Coulter Laser Diffraction Particle Size Analyzer (LS13320).

### 258 3.4 Measurement of carbon and nitrogen element and their stable isotopes

259 Samples for total organic carbon (TOC), total nitrogen (TN), δ<sup>13</sup>C and δ<sup>15</sup>N  
260 analysis were firstly freeze-dried, milled and sieved with a 74 μm (200 mesh) sieve.  
261 The fine fraction was collected and a subsample treated with 1M HCl to remove  
262 carbonate followed by washing for four to five times with distilled water before  
263 drying in an oven at 45 °C. Samples without additional treatment of HCl were used to  
264 measure TC and TN, whilst carbonate-free samples were analysed for TOC and  
265 isotopic carbon and nitrogen (Zhang et al., 2007).

266 TC, TOC and TN were measured using an organic element analyzer (Carlo-Erba  
267 model EA1110, Italy) in the State Key Laboratory of Marine Geology at Tongji  
268 University, China. TOC concentration was calibrated with equation (1) (Yang et al.,  
269 2011):

$$270 \quad \text{TOC (\%)} = \text{TOC}_{\text{measured}} (\%) \times (12 - \text{TC (\%)}) / (12 - \text{TOC}_{\text{measured}} (\%)) \quad (1)$$

271 TOC/TN refers to the weight ratio of TOC (%) to TN (%) in this paper. Stable  
272 isotopic carbon and nitrogen were measured using a Thermo Deltaplus XL mass  
273 spectrometer (continuous flow mode) at the Third Institute of Oceanography, State  
274 Oceanic Administration, China. The stable isotopic ratios were expressed as δ<sup>13</sup>C and

275  $\delta^{15}\text{N}$ , in standard units per mil (‰), with respect to PeeDee Belemnite (PDB) and  
276 atmospheric nitrogen, respectively. The standard samples used for carbon and  
277 nitrogen isotope measuring referred to Urea#2 and Acetanilide#1 from  
278 Biogeochemistry Laboratories Indiana University. The precision for  $\delta^{13}\text{C}$  and  $\delta^{15}\text{N}$   
279 were  $< 0.2$  ‰ and  $< 0.3$  ‰, respectively, based on replicated measurements ( $n = 5$ ).

280 TOC/TN ratio and their isotopes are widely used to trace the source of organic  
281 matter in lakes and river-estuary-marine systems (Müller and Mathesius, 1999;  
282 Meyers, 2003; Wilson et al., 2005; Lamb et al., 2007; Leng and Lewis, 2017).  
283 Previous studies have found that TOC/TN ratios are  $> 12$ , 4-6, and  $< 10$  for terrestrial  
284 vegetation, bacteria, and algae respectively (in Müller and Mathesius, 1999; Lamb et  
285 al., 2007; Leng and Lewis, 2017 and references).  $\delta^{13}\text{C}$  values are in a range of  $-21$  to  
286  $-31$  ‰,  $-20$  to  $-30$  ‰,  $-17$  to  $-22$  ‰ for typical terrestrial  $\text{C}_3$  plants, freshwater  
287 plankton, and marine plankton respectively (Müller and Voss, 1999 and references in;  
288 Lamb et al., 2007; Leng and Lewis, 2017 and references in). Terrestrial plants usually  
289 have relative low  $\delta^{15}\text{N}$  values compared with aquatic plankton (Thornton and  
290 McManus, 1994; Middelburg and Nieuwenhuize, 1998; Müller and Voss, 1999).  
291 These values are the underlying principles on which we base our interpretation of  
292 TOC/TN,  $\delta^{13}\text{C}$  and  $\delta^{15}\text{N}$  profiles in cores DTX4 and DTX10.

### 293 *3.5 Collection of previous archive cores and palaeogeographic reconstruction of the* 294 *Taihu Plain*

295 To correlate morphological and hydrological conditions in the East Tiaoxi River  
296 Plain to other parts of the Taihu Plain and reconstruct palaeohydrological conditions  
297 of the whole Taihu Plain, previously published borehole records were compiled,  
298 selecting only those which have good chronological (radiocarbon age) control. In total,  
299 23 sediment cores were selected and subdivided into 3 sections A-A', B-B' and C-C'

300 (Fig. 1A and 1C) to make stratigraphic comparisons (core details including location,  
301 dating depth, dating material, dating results and references are provided in  
302 [Supplementary Table 1](#)). Conventional ages in these cores were calibrated in software  
303 Calib 7.0 ([Talma and Vogel, 1993](#)) using the INTCAL 13 database where dating  
304 materials were plant fragments, organic rich mud, seeds, wood and pollen residues,  
305 and the Marine 13 database and  $\Delta R$  value of  $135 \pm 42$  when dating materials were  
306 marine molluscs ([Yoneda et al., 2007](#); [Reimer et al., 2013](#)). A linear interpolation  
307 method was used to construct ages for key depths, based on the program ‘Clam’ with  
308 10,000 iterations ([Blaauw, 2010](#)).

309 Using sedimentary, morphological and hydrological changes obtained in our new  
310 cores (DTX10 and DTX4 presented here) together with those inferred in the 23  
311 selected existing cores, stratigraphic transections for the sections A-A’, B-B’ and C-C’  
312 were reconstructed. Accordingly, sedimentary morphological and hydrological  
313 conditions across the whole Taihu Plain were reconstructed for several periods  
314 between ca. 7500 and ca. 5500 cal. yr BP, associated with palaeotopography contexts  
315 during the LGM ([Fig. 1C](#); [Hong, 1991](#); [Li et al., 2002](#); [Wang et al., 2012](#)) and relative  
316 sea-level changes in the Yangtze delta during the Holocene ([Zong, 2004](#); [Wang et al.,](#)  
317 [2012, 2013](#)).

318

## 319 **4. Results and interpretation**

320 *4.1 Lithology, AMS <sup>14</sup>C dating and sedimentary accumulation rates in cores DTX4*  
321 *and DTX10*

322 *4.1.1 Core DTX4*

323 The bottom 2.7 m of the sequence (i.e. 5.7-3.0 m depth) consisted of grey  
324 homogeneous mud with abundant plant fragments ([Fig. 2](#)). This changed to dark,

325 organic-rich mud over 3.0-2.0 m, followed by a peaty mud layer (2.0-1.8 m). Grey  
326 homogeneous mud with abundant plant fragments reoccurred at 1.8-1.45 m, with  
327 peaty mud at 1.75 and 1.5-1.45 m. Plant fragments declined from 1.45 m to the top. In  
328 total, six AMS <sup>14</sup>C dates were obtained over the sequence (Table 1). These ages are in  
329 reasonable sequential order with the exception of the date obtained at 1.21 m, which is  
330 older than the age obtained from the peaty mud at 1.45 m. We reject this reversed age  
331 because it could be derived from reworked plant macrofossils. By contrast, the age  
332 from peaty mud is more reliable because the peaty mud was formed by *in situ*  
333 deposition of local marsh plants. Stanley (2000) reported that it is quite common that  
334 radiocarbon dates of Holocene sediments do not become progressively older with  
335 depth in cores from the Yangtze delta, due to the introduction of old carbon during  
336 sediment transport and storage. This ‘old carbon’ phenomenon has also been  
337 discussed by Wang et al. (2012). The remaining five dates were used to generate the  
338 linear interpolation age-depth model and to calculate sedimentation rate (SR) with the  
339 program ‘Clam’ (Blaauw, 2010; Fig. 2). Relatively high SR of 0.47 cm per year (cm  
340 yr<sup>-1</sup>) from 7050 to 6450 cal. yr BP (5.33-2.5 m) was followed by a reduced SR of  
341 0.056 cm yr<sup>-1</sup> from 6450-5560 cal. yr BP (2.5-1.91 m) and 0.004 cm yr<sup>-1</sup> from  
342 5560-2990 cal. yr BP (1.91-1.81 m). After 2990 cal. yr BP, SR increased to 0.017  
343 from 1.81-1.45 m and to 0.072 from 1.45-0.8 m (Fig. 2).

#### 344 4.1.2 Core DTX10

345 From the base of the sequence (4.7 m) to 1.0 m, lithology was grey  
346 homogeneous mud with plant fragments occurring occasionally (Fig. 2). This changed  
347 to light grey homogeneous, stiff mud with bluish leaching structures at 1.0-0.88 m,  
348 indicating subaerial pedogenesis processes and hence a sedimentation hiatus. At 0.88  
349 m, it became dark, homogeneous mud with abundant plant fragments to the top. Four



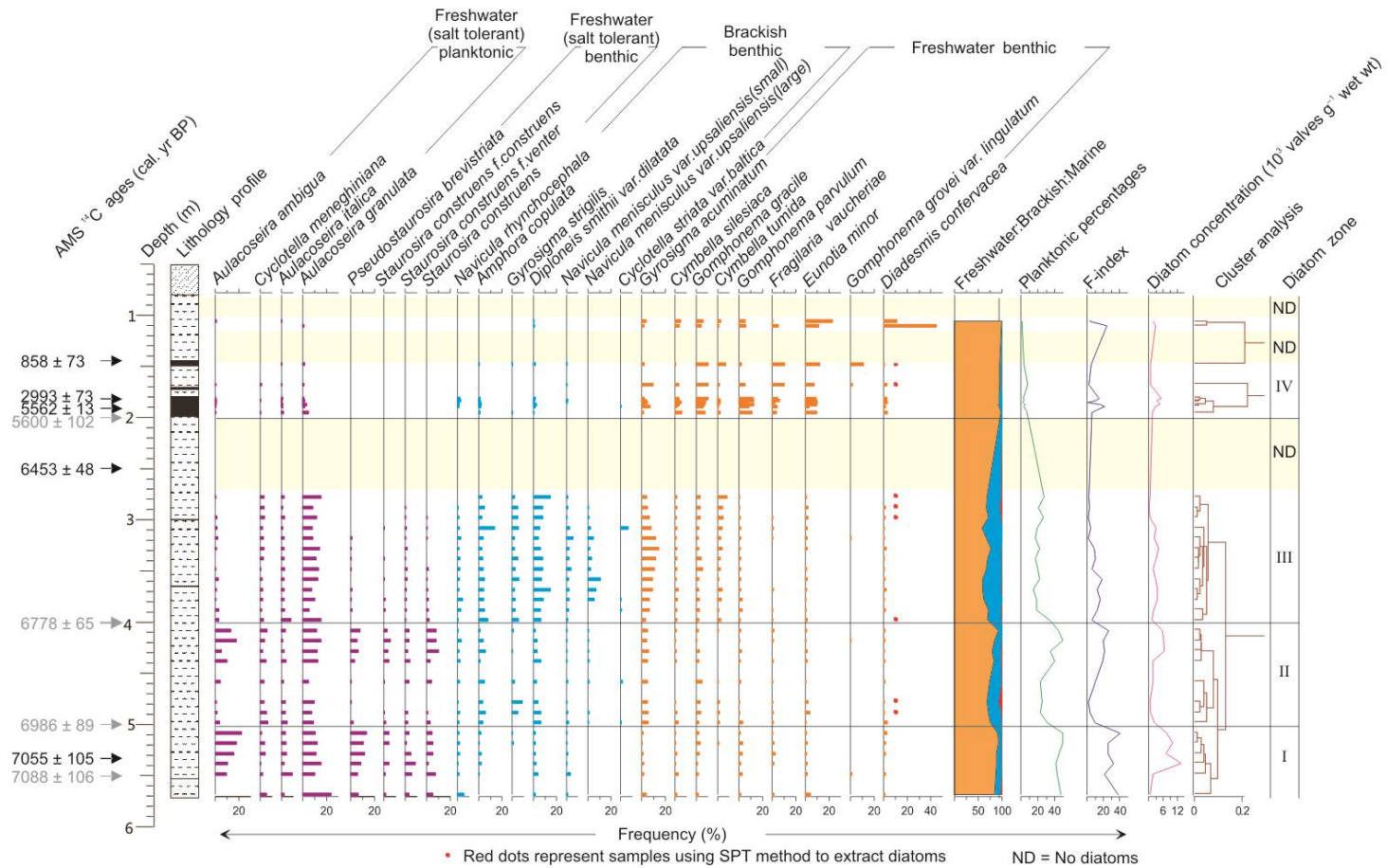
350 AMS  $^{14}\text{C}$  dates were obtained throughout the sequence (Table 1). The reversed date at  
351 2.91 m (9475-9400 cal. yr BP) was rejected, as we argue that it was also derived from  
352 reworked plant material as discussed earlier (Stanley, 2000; Wang et al., 2012). The  
353 remaining three dates were used to construct the age-depth model and to calculate SR  
354 based on ‘Clam’ (Fig. 2). When running the age-depth model in ‘Clam’, a  
355 sedimentation hiatus was set at 1.0 m, as reflected by the pedogenesis at 1.0-0.88 m.  
356 Core DTX10 showed similar SR pattern to core DTX4. Before 7460 cal. yr BP (below  
357 1 m), SR was high (up to  $2\text{ cm yr}^{-1}$ ), thereafter pedogenesis and a sedimentation  
358 hiatus occurred from 7460 to 2810 cal. yr BP (1.0-0.88 m). Following this, SR rose to  
359  $0.03\text{ cm yr}^{-1}$  after 2810 cal. yr BP (0.88-0 m).

#### 360 *4.2 Diatom assemblages*

##### 361 *4.2.1 Core DTX4*

362 A total of 236 species were identified and four habitat groups were distinguished  
363 including freshwater, salt-tolerant freshwater, brackish and marine species. No  
364 diatoms were found from 2.0-2.75 m and 1.2-1.45 m. All diatom species  $> 5\%$  were  
365 plotted as percentages of the total assemblage in Figure 3.

366



367

368 **Fig. 3** Diatom taxa in core DTX4 (> 5 % relative abundance) separated into freshwater (including both freshwater and salt-tolerant freshwater groups), brackish, and marine species,  
 369 percentages of planktonic species, F-index and diatom concentration. Calibrated AMS <sup>14</sup>C dates (in dark) and calculated age regions (in grey) for important boundaries are presented as  
 370 ‘medial point ages ± standard deviation’, as in Figures 4, 5 and 7.

371 In Zone I (5.7-5.0 m, 7140-6990 cal. yr BP), diatom concentration was the  
372 highest over the whole sequence (avg.  $6.84 \times 10^3$  valve  $g^{-1}$  wet weight). On the  
373 contrary, F-index was the highest, with 29.1 % of valves on average remaining in  
374 pristine state (Fig. 3). The two most abundant species were *Aulacoseira granulata*  
375 (avg. 13.8 %) and *Aulacoseira ambigua* (avg. 12.6 %). These two salt-tolerant  
376 freshwater planktonic species with low salt tolerance favour shallow fresh water (low  
377 salinity tolerant) and well-mixed hydrological conditions (Kilham, 1990; Owen and  
378 Crossley, 1991). Freshwater benthic species such as *Pseudostaurosira brevistriata*  
379 (avg. 9.2 %), *Staurosira construens* (avg. 4.9 %) and its varieties of *Staurosira*  
380 *construens f. venter* (avg. 4.3 %) and *Staurosira construens f. construens* (avg. 2.5 %)   
381 followed. Brackish benthic (e.g. *Diploneis smithii* var. *dilatata*, *Amphora copulata*)  
382 and freshwater benthic species (e.g. *Gomphonema gracile/parvulum*, *Eunotia minor*)  
383 were also found, but at low percentages (less than 3 % for each). The average  
384 percentage of freshwater species (including both freshwater and freshwater with low  
385 salt tolerance groups) in this section was 88.5 % while brackish species accounted for  
386 only 9.9 %, and the average percentage of planktonic species was 39.5 %.

387 In Zone II (5.0-4.0 m, 6990-6780 cal. yr BP), the diatom concentration decreased  
388 to  $3.23 \times 10^3$  valve  $g^{-1}$  wet weight, while the F-index declined slightly to 13.9 %.  
389 Relative concentration of freshwater planktonic (e.g. *A. ambigua*) and freshwater  
390 benthic with low salt tolerance species (e.g. *P. brevistriata*, *S. construens* and its  
391 varieties of *S. construens f. venter* and *S. construens f. construens*) decreased slightly,  
392 with the exception of *A. granulata* which remained fairly constant. Correspondingly,  
393 percentages of brackish and freshwater benthic species (including *D. smithii* var.  
394 *dilatata*, *A. copulata*, *Gyrosigma acuminatum*, *G. gracile*) rose slightly. A brief  
395 recovery of the low salinity planktonic (*A. ambigua/granulata*) and benthic (*P.*  
396 *brevistriata*, *S. construens* and its varieties) group occurred at the top of this unit

397 (4.0-4.4 m). The average percentages of freshwater species dropped to 78.5 % while  
398 brackish species rose to 19.3 %, and planktonic species decreased to 29.5 %.

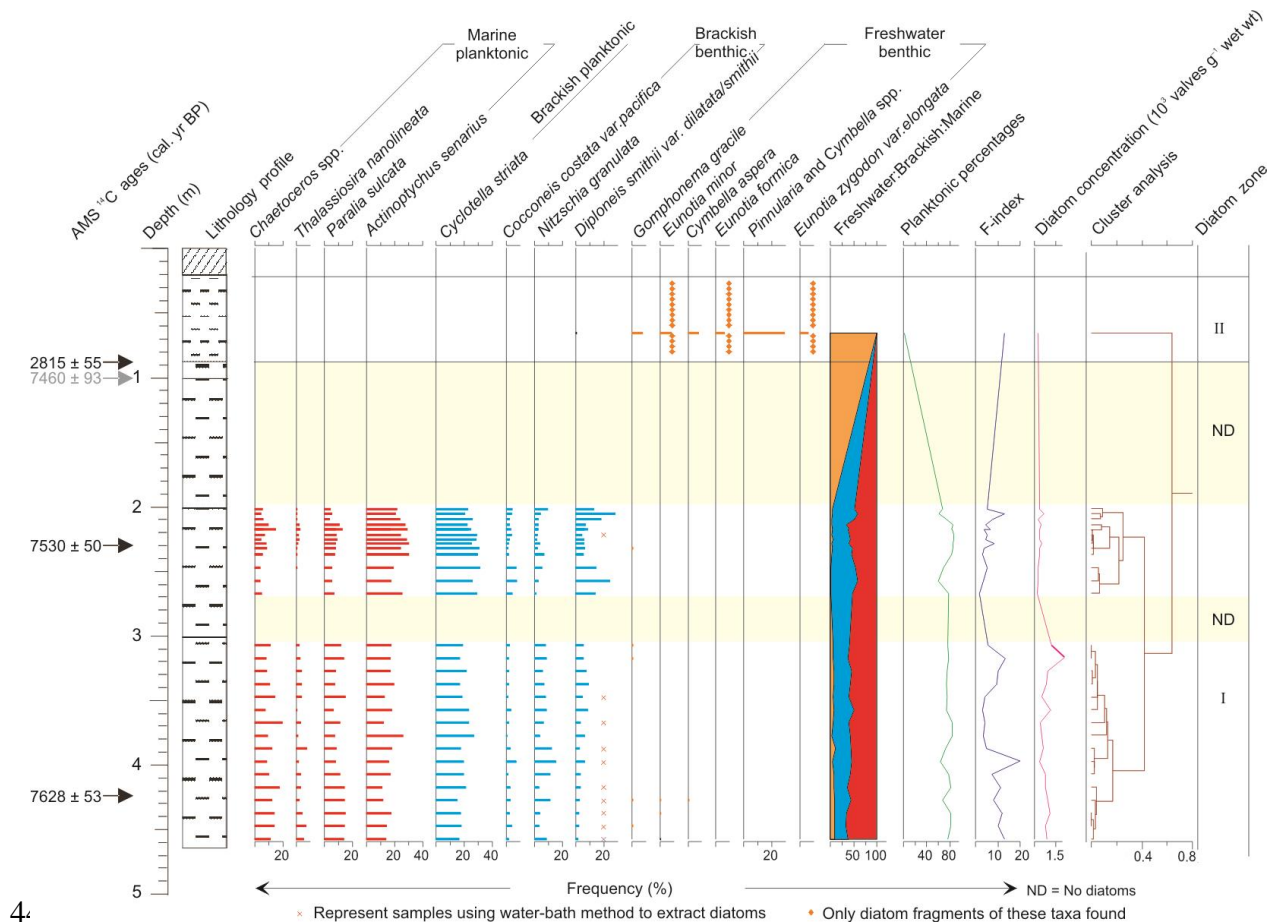
399 In Zone III (4.0-2.7 m, 6780-6500 cal. yr BP), a further drop of diatom  
400 concentration (avg.  $2.23 \times 10^3$  valve  $g^{-1}$  wet weight) occurred, accompanied by  
401 increasing dissolution (F-index dropped to 7.9 %). *A. granulata* remained relatively  
402 abundant (avg. 10.8 %), despite a further decrease in the low salinity assemblages,  
403 giving way to brackish benthic (e.g., *D. smithii* var. *dilatata*, *A. copulata*, *Gyrosigma*  
404 *strigilis* and *Navicula menisculus*) and freshwater benthic (e.g. *G. accuminatum*, *G.*  
405 *gracile*, *Cymbella tumida*) species. The average percentage of freshwater species  
406 declined to 66.7 % and brackish species rose to 31.6 %, with the planktonic group  
407 falling to 20.4 %.

408 A remarkable shift in the diatom assemblage occurred in Zone IV (2.0 m from  
409 the top, 5570 cal. yr BP to the present), associated with a slight increase in diatom  
410 concentration (avg.  $2.85 \times 10^3$  valve  $g^{-1}$  wet weight) and increase in F-index (avg.  
411 9.7 %). This unit was dominated by freshwater benthic and epiphytic species of *G.*  
412 *parvulum/gracile*, *E. minor*, *Fragilaria vaucheriae* and *Cymbella silesiaca*, with  
413 very few brackish benthic (e.g. *D. smithii* var. *dilatata*, *A. copulata*, *N. menisculus*, *G.*  
414 *strigilis*) and freshwater to low salinity tolerant planktonic species (e.g. *A.*  
415 *granulata/ambigua*). In the uppermost samples (1.1-1.0 m), *Diadesmis confervacea*  
416 became frequent (up to 45 %), an indicator of aerial/terrestrial or very shallow-water  
417 conditions (Gell et al., 2007). Freshwater species accounted for 95.1 % and brackish  
418 species were < 5 % on average, while planktonic species accounted for only 3.9 % of  
419 the assemblage.

#### 420 4.4.2 Core DTX10

421 Diatom concentration was low with an average value of  $0.46 \times 10^3$  valve  $g^{-1}$  wet  
422 weight for the whole core (Fig. 4), probably resulting from strong dissolution of  
423 diatoms reflected by low average F-index value ( $\sim 7.4$  %) and dilution caused by high  
424 sediment accumulation rates or low diatom productivity. No diatoms were found from  
425 2.7-3.0 m and 0.84-2.0 m and only a few broken diatom fragments were found on  
426 slides for samples from the top to 0.84 m. Preservation in one sample at 0.66 m was  
427 slightly better, but most remaining diatoms were the dissolved centres of large benthic  
428 genera *Pinnularia* or *Cymbella*, but which cannot be identified to species level. For  
429 other samples from 0.3 to 0.84 m, broken fragments of freshwater genera, such as  
430 *Eunotia* species, were seen. A total of 154 species were identified for the whole  
431 sequence and diatom species  $> 5$  % plotted as relative abundance in Figure 4.

432 The diatom assemblage from the base to 2.0 m (7650-7520 cal. yr BP; except  
433 2.7-3.0 m where no diatoms were found) was dominated by *Cyclotella striata* (avg.  
434 22.5 %), which is usually abundant in river-mouth/estuarine environments (Ryu et al.,  
435 2005), *Actinoptychus senarius* (avg. 19.8 %), the relatively low-salinity coastal  
436 planktonic species (Grönlund, 1993; Hasle and Syvertsen, 1996), *Paralia sulcata* (avg.  
437 9.3 %) which is used as a marker for the coastal East China Sea (Tada et al., 1999.  
438 Ryu et al., 2005), and *Chaetoceros spp.* resting spores, typical marine species (avg.  
439 9.2 %). Other species found but in relatively low percentage were coastal species of  
440 *Thalassiosira nanolineata* (Grönlund, 1993; Hasle and Syvertsen, 1996) and brackish  
441 benthic species such as *Diploneis smithii* var. *dilatata/smithii*, *Nitzschia granulata*,  
442 *Cocconeis costata* var. *pacifica*. In total, percentages of marine and brackish species  
443 were 56.3 % and 37.9 % on average respectively, and planktonic species 77.4 %  
444 (including tychoplanktonic taxa).



446 **Fig. 4** Diatom taxa in core DTX10 (> 5 % relative abundance) with separated into freshwater,  
 447 brackish and marine species, percentages of planktonic species, F-index and diatom concentration.

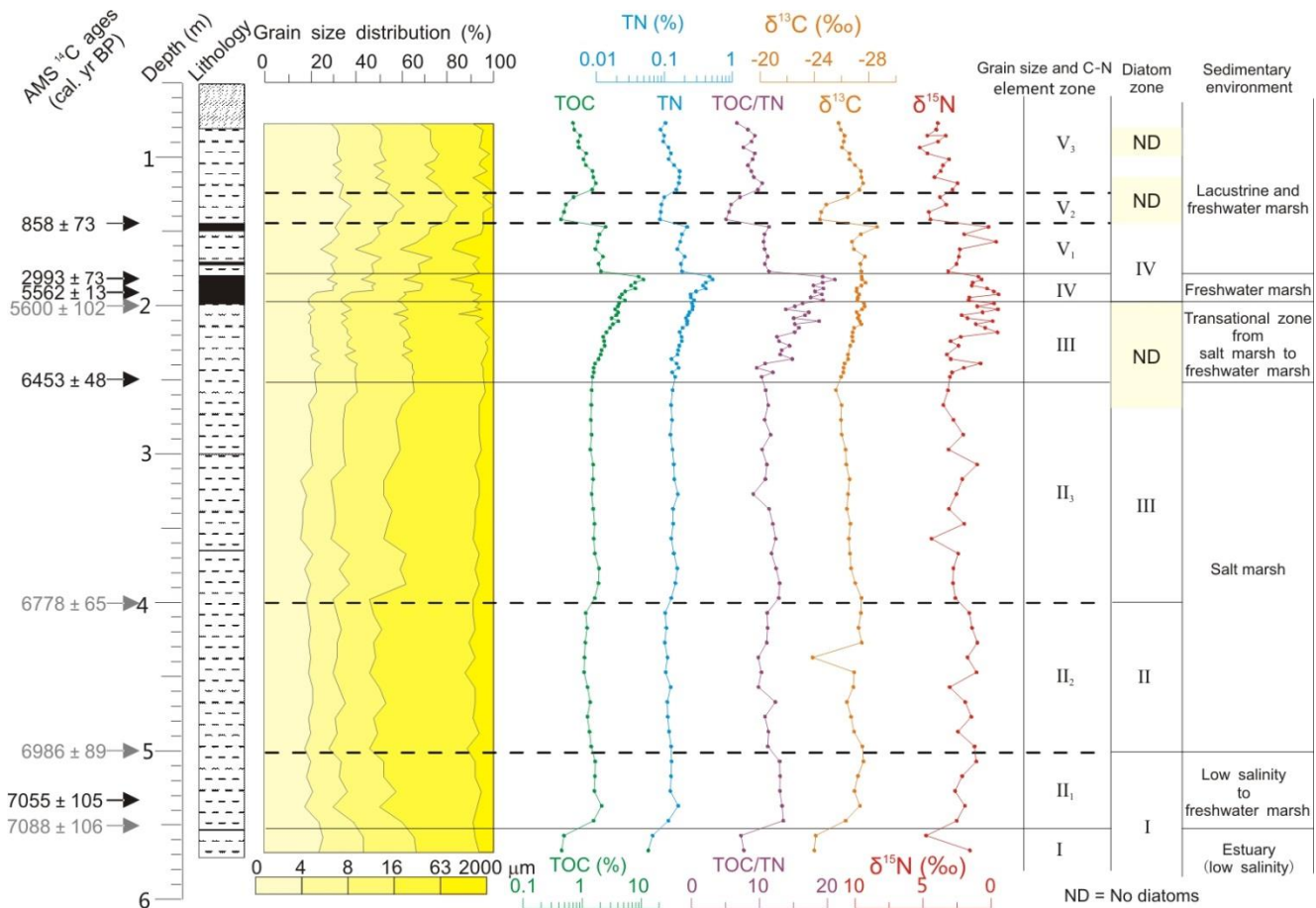
448  
 449 Although preservation was very poor in samples from the top to 0.84 m, it was  
 450 clear that the original diatom assemblage was completely different. Almost 99% of  
 451 diatom valves (as represented by the sample at 0.66 m) belonged to freshwater benthic  
 452 species (including *Gomphonema gracile*, *Cymbella aspera*, *Eunotia minor*, *E.*  
 453 *formica* and unidentified *Pinnularia* and *Cymbella* species). We argue that the switch  
 454 from a brackish/marine to a freshwater assemblage from Zone I to Zone II reflects a  
 455 real change to the salinity and hydrology of the system as the vestigial fragments of  
 456 diatoms in Zone II are resistant and have distinctive morphologies. Had these taxa

457 been part of the assemblage of earlier sections, they would have been significant  
458 aspects of the assemblages there also. By the same token, most of the taxa in the  
459 earlier, more marine parts of Zone I are also very resistant to dissolution (e.g.  
460 *Chaetoceros* cysts, *Paralia sulcata*, *Cyclotella striata*) with distinctive taphonomic  
461 end-members, and would have appeared in Zone I had they been present in the  
462 original assemblage in that section. Thus we are confident that Zone I was deposited  
463 under brackish-marine conditions while Zone II represents a freshwater system.

#### 464 *4.3 Grain size, TOC/TN ratio and C-N stable isotopes*

465 Based on grain size composition, TOC, TN, TOC/TN and C-N stable isotope  
466 ( $\delta^{13}\text{C}$ ,  $\delta^{15}\text{N}$ ) variations, cores DTX4 and DTX10 were divided into five and three  
467 zones, denoted as Zone I-V, respectively (Figs 5-7). Zone II and V in core DTX4 (Fig.  
468 5) were both divided into three sub-zones based on variation of TOC/TN ratio,  $\delta^{13}\text{C}$   
469 and  $\delta^{15}\text{N}$  values. Zone I and III in core DTX10 were also divided into three and two  
470 sub-zones respectively.

471



473 **Fig. 5** Lithology and sedimentary parameters of core DTX4, including AMS <sup>14</sup>C age, grain size  
 474 distribution, TOC, TN, TOC/TN,  $\delta^{13}\text{C}$ ,  $\delta^{15}\text{N}$ , and interpretation of sedimentary environment.

475 **4.3.1 Core DTX4**

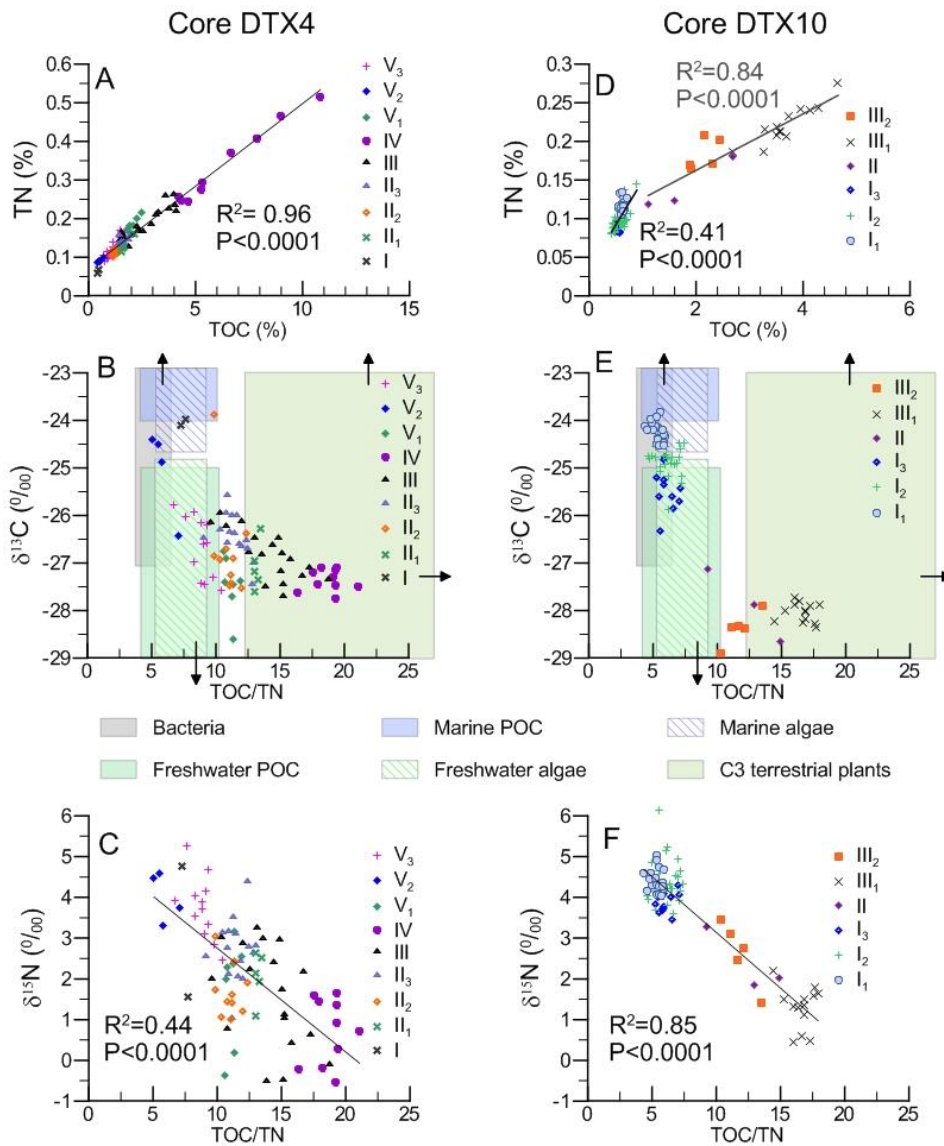
476 In Zone I (5.7-5.5 m, 7140-7100 cal. yr BP), clay content ( $< 4 \mu\text{m}$ ) was around  
 477 24.8 %, silt (4-63  $\mu\text{m}$ ) 67.7 %, and sand (63-2000  $\mu\text{m}$ ) 7.3 % on average. In Zone II  
 478 (5.5-2.5 m, 7100-6450 cal. yr BP), clay content (avg. 19.6 %) decreased and silt  
 479 content (avg. 72.7 %) increased slightly, particularly for grains between 16 and 63  $\mu\text{m}$ .  
 480 No change occurred in sand content. Particles between 8-16  $\mu\text{m}$  increased slightly  
 481 while particles between 16-63  $\mu\text{m}$  fell in  $\text{II}_3$  (4.0-2.5 m, 6780-6450 cal. yr BP)  
 482 compared to  $\text{II}_1$  (5.5-5.0 m, 7100-6990 cal. yr BP) and  $\text{II}_2$  (5.0-4.0 m, 6990-6780 cal.



483 yr BP). Grain size assemblages in Zone III (2.5-2.0 m, 6450-5570 cal. yr BP)  
484 remained similar to those of Zone II, followed by a sudden increase in sand content in  
485 Zone IV (2.0-1.8 m, 5570-2990 cal. yr BP) and clay content in Zone V (1.8 m to the  
486 top, 2990 cal. yr BP to the present) with an opposite trend in silt content.

487 The linear correlation of TOC to TN (Fig. 6A) implied that TN content was  
488 controlled mostly by organic matter, while the positive TN intercept of 0.07 %  
489 indicated a slight contribution from inorganic nitrogen. Plots of  $\delta^{13}\text{C}$  and  $\delta^{15}\text{N}$  against  
490 TOC/TN revealed a mixture of freshwater and marine algae and terrestrial  $\text{C}_3$  plants  
491 (Fig. 6B and 6C). In Zone I, TOC (avg. 0.47 %), TN (avg. 0.06 %) and TOC/TN (avg.  
492 7.48) minima coincided with relatively high  $\delta^{13}\text{C}$  (avg.  $-24.04$  ‰) and  $\delta^{15}\text{N}$  (avg.  
493  $+3.16$  ‰), indicating contribution from marine plankton and bacteria (Müller and  
494 Mathesius, 1999; Müller and Voss, 1999; Lamb et al., 2007). The bi-plot of  $\delta^{13}\text{C}$  to  
495 TOC/TN showed that Zone I samples lay in the domain of marine algae or marine  
496 particulate organic carbon (POC; Fig. 6B). The bi-plot of  $\delta^{15}\text{N}$  against TOC/TN  
497 reflected a predominant contribution from algae as well (Fig. 6C).

498 An abrupt increase in TOC (1.07-2.12 %, avg. 1.47 %), TN (0.10-0.16 %, avg.  
499 0.13 %) and TOC/TN (9.07-13.50, avg. 11.53) characterised zone II with lower  $\delta^{13}\text{C}$   
500 (from  $-25.58$  ‰ to  $-26.61$  ‰, avg.  $-26.74$  ‰) and  $\delta^{15}\text{N}$  (from  $+1$  ‰ to  $+4.39$  ‰, avg.  
501  $+2.25$  ‰), signifying the sudden increase in importance of  $\text{C}_3$  terrestrial plants and  
502 reflecting the formation of a marsh environment. A shift on the bi-plots of  $\delta^{13}\text{C}$  and  
503  $\delta^{15}\text{N}$  vs. TOC/TN implied a mixture of freshwater POC and  $\text{C}_3$  plants for samples in  
504 Zone II with one exception of marine POC in Zone II<sub>2</sub>. The gradual increase in  $\delta^{13}\text{C}$   
505 and  $\delta^{15}\text{N}$  from Zone II<sub>1</sub> to II<sub>2</sub>, and to II<sub>3</sub>, coincided with changes in position in bi-plots  
506 of  $\delta^{13}\text{C}$  and  $\delta^{15}\text{N}$  against TOC/TN which was interpreted as a slight, but persistent,  
507 increase in the importance of marine algae/POC from the bottom to the top of Zone II.



508

509 **Fig. 6** Correlation between TOC and TN (A and D), biplot of  $\delta^{13}C$  values and TOC/TN (B and E),  
 510 correlation between  $\delta^{15}N$  values and TOC/TN (C and F) for core DTX4 (A to C) and DTX10 (D to F),  
 511 respectively. Regions for different type of organic matter are after Lamb et al. (2007).

512 TOC, TN, TOC/TN values increased gradually to maxima of 10.83 %, 0.51 %  
 513 and 21.09, respectively, from Zone III to the top of IV where lithology changed to  
 514 peaty mud, while  $\delta^{13}C$  and  $\delta^{15}N$  values dropped consistently to minima of  $-27.76$  ‰  
 515 and  $-0.55$  ‰, respectively. Integrating patterns on the two bi-plots (Fig. 6B and 6C),

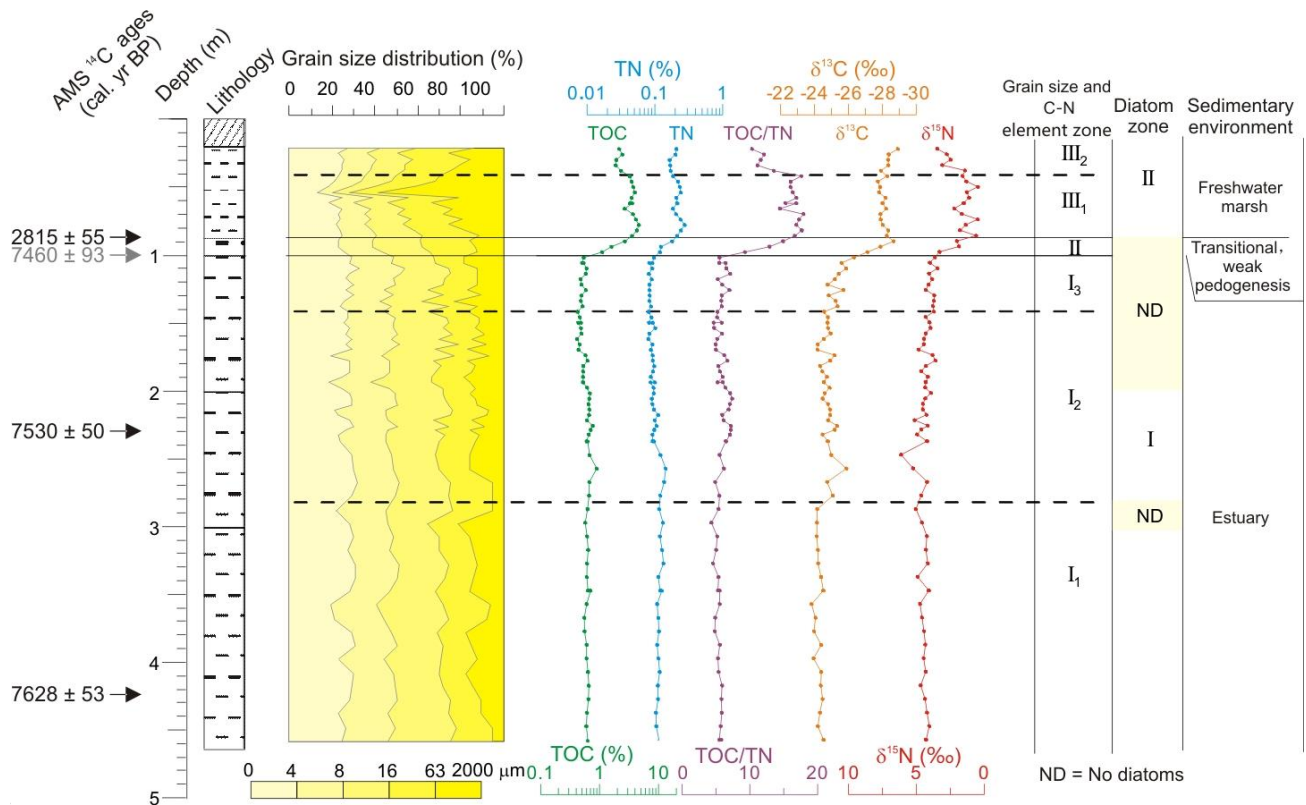
516 Zone III was dominated mostly by terrestrial C<sub>3</sub> plants and secondarily by freshwater  
517 algae/POC, while typical terrestrial C<sub>3</sub> plants dominated the organic matter  
518 composition of Zone IV. In Zone V, a rapid drop in TOC (avg. 1.34 %), TN (avg.  
519 0.14 %) and the TOC/TN ratio (avg. 9.13) occurred, with lowest values in subzone V<sub>2</sub>  
520 followed by an increase in subzone V<sub>3</sub>. The δ<sup>13</sup>C values remained depleted except for  
521 subzone V<sub>2</sub> (1.25-1.45 m) where they showed peaks, while the δ<sup>15</sup>N values increased  
522 suddenly and remained high from the bottom to the top. The pattern on the two  
523 bi-plots (Fig. 6B and 6C) suggested an increase in freshwater algae/POC and bacteria  
524 in Zone V, especially in Zone V<sub>2</sub> where algae and bacteria dominated.

525

#### 526 4.3.2 Core DTX10

527 In Zone I (from the base to 1.0 m, 7650-7460 cal. yr BP), silt content was  
528 50-74 %, the highest values in the profile, with lesser amounts of clay and sand (Fig.  
529 7). Zone II (1.0-0.88 m, 7460-2810 cal. yr BP) was a transitional zone for all proxies.  
530 There was a slight and gradual increase in silt content from the bottom to the top,  
531 while sand content remained constant. In Zone III (0.88 m to the top, 2810 cal. yr BP  
532 to present) both silt and clay content dropped while sand content rose dramatically to  
533 26 % on average, with a slight increase in clay and silt content at the top of Zone III<sub>2</sub>.

534



536 **Fig. 7.** Lithology and sedimentary parameters of core DTX10, including AMS  $^{14}\text{C}$  age, grain size  
 537 distribution, TOC, TN, TOC/TN,  $\delta^{13}\text{C}$ ,  $\delta^{15}\text{N}$ , and sedimentary environments interpretation.

538 A linear correlation between TOC and TN was found, but two discrete groups  
 539 were identified (Fig. 6D): the samples in Zone I formed one group and samples in  
 540 Zone II and III a second. This showed that TN values were mostly controlled by  
 541 organic matter, but also inorganic nitrogen contributed slightly as shown by the  
 542 positive TN intercept of 0.035 % and 0.09 % respectively. Plotting  $\delta^{13}\text{C}$  against  
 543 TOC/TN revealed a mixture of two end members of POC/algae/bacteria and  $\text{C}_3$   
 544 terrestrial plants (Fig. 6E). This explanation was supported by the strongly negative  
 545 linear correlation between  $\delta^{15}\text{N}$  and TOC/TN ( $r = -0.85$ ; Fig. 6F). TOC values were  
 546 0.42-0.89 % (avg. 0.59 %) in zone I and TN 0.08-0.14 % (avg. 0.10 %) (Fig. 7), while  
 547 TOC/TN ratios were 4.35-7.41 (avg. 5.80). These minimum values were accompanied

548 by the highest  $\delta^{13}\text{C}$  (from  $-23.82\text{‰}$  to  $-26.32\text{‰}$ , avg.  $-24.73\text{‰}$ ) and  $\delta^{15}\text{N}$  values  
549 (from  $+3.44\text{‰}$  to  $+6.12\text{‰}$ , avg.  $4.30\text{‰}$ ). Very small increases in TOC, TN and  
550 TOC/TN coincided with minor decreases of  $\delta^{13}\text{C}$  and  $\delta^{15}\text{N}$  from Zone I<sub>1</sub> to I<sub>3</sub>.  
551 Integrating patterns on the plots of  $\delta^{13}\text{C}$  and  $\delta^{15}\text{N}$  against TOC/TN, a mixture of  
552 freshwater and marine algae/POC and bacteria composed the organic matter source  
553 for samples in Zone I, with the freshwater algal/POC contribution increasing from  
554 Zone I<sub>1</sub> to I<sub>3</sub>. In Zone II, TOC and TN values increased rapidly up to 1.79 % and 0.14 %  
555 on average and TOC/TN up to 12.37. On the contrary,  $\delta^{13}\text{C}$  and  $\delta^{15}\text{N}$  declined to  
556  $-27.89\text{‰}$  and  $+2.39\text{‰}$ , respectively. Changes in all these proxies reflected an abrupt  
557 addition of terrestrial organic matter from C<sub>3</sub> plants, supported by the bi-plots of  $\delta^{13}\text{C}$   
558 and  $\delta^{15}\text{N}$  against TOC/TN. In Zone III, this pattern of consistently high TOC, TN and  
559 TOC/TN and lower  $\delta^{13}\text{C}$  and  $\delta^{15}\text{N}$  continued, with small decreases in these  
560 parameters in Zone III<sub>2</sub>. On bi-plots of  $\delta^{13}\text{C}$  and  $\delta^{15}\text{N}$  vs. TOC/TN, samples of Zone  
561 III<sub>1</sub> fell in the region typical of C<sub>3</sub> terrestrial plants and samples of Zone III<sub>2</sub> in the  
562 region between C<sub>3</sub> plants and freshwater POC/algae.

563

## 564 **5. Discussion**

### 565 *5.1 Sedimentary, morphological and hydrological changes in the East Tiaoxi River* 566 *Plain*

567 The dominance of marine diatoms and marine algae/POC contribution for the  
568 TOC in core DTX10 confirms that there was a high salinity estuary (the Palaeo-Taihu  
569 Estuary) in the East Tiaoxi River Plain before ca. 7500 cal. yr BP (Figs 4, 7; Hong,  
570 1991), in response to rapid early to mid-Holocene sea-level rise (Chappell and Polach,  
571 1991; Bard et al., 1996; Bird et al., 2007; Wang et al., 2012). The high sedimentation  
572 accumulation rate up to 2 cm yr<sup>-1</sup> in core DTX10 during this period signified rapid

573 infilling of this estuary. From ca. 7500 cal. yr BP, freshening occurred at site DTX10  
574 indicated by the increase in organic source from freshwater algae/POC (Zone I<sub>2</sub>-I<sub>3</sub> in  
575 Fig. 7). At some time after ca. 7500 cal. yr BP, the area around core DTX10 was  
576 subaerially exposed until ca. 2800 cal. yr BP, inferred from the sedimentation hiatus  
577 and observed pedogenesis (1.0-0.88 m in Fig. 2 and 7). In contrast, the area around  
578 core DTX4 changed from estuary to a low-salinity marsh during ca. 7100-7000 cal. yr  
579 BP, indicated by dominant organic matter changing from marine algae/POC to  
580 freshwater algae/POC and C<sub>3</sub> terrestrial plants (Fig. 5). The estuary at 7100 cal. yr BP  
581 was also characterised by low salinity, with the diatom assemblages dominated by  
582 salt-tolerant freshwater group of *A. granulata/ambigua*, *P. brevistriata*, *S. construens*  
583 and its varieties of *S. construens f. venter* and *S. construens f. construens* (Fig. 3).  
584 These diatom taxa are often found in isolation basins (e.g. freshwater lakes formed as  
585 sea level falls) (Stabell, 1985), and therefore, their high concentrations indicate that  
586 the site DTX4 was in the stage of isolation from seawater during ca. 7100-7000 cal. yr  
587 BP. Consequently, we infer that the freshening of the East Tiaoxi River Plain likely  
588 started between 7500-7100 cal. yr BP, possibly due to coastal development and  
589 freshwater discharge from the Yangtze River, benefitting from a warmer and, more  
590 importantly, wetter climate during the Holocene Thermal Maximum (Wang et al.,  
591 2005). Particularly, *A. granulata* is often found in rivers/lakes in the flood and delta  
592 plains in eastern China and has been considered as an indicator of freshwater  
593 discharge to estuaries (Chen et al., 2011; Dong et al., 2008; Liu et al., 2012; Wang et  
594 al., 2009). We thus suppose high and constant percentages of *A. granulata* during  
595 7100-6500 cal. yr BP in core DTX4 implied the strong freshwater influence of  
596 Yangtze River runoff.

597         At some time after ca. 7000 cal. yr BP, although the marsh was dominated by C<sub>3</sub>  
598 plants and strongly influenced by the Yangtze freshwater discharge, penetration of salt

599 water occurred at core DTX4 as percentages of brackish benthic diatom and influence  
600 from marine POC/algae increased (Zone II<sub>2</sub> and II<sub>3</sub> in Fig. 5; Fig. 6). During this  
601 period, the infilling of the Palaeo-Taihu Estuary continued, but at a lower SR of 0.48  
602 cm yr<sup>-1</sup>. The return of sea water was likely caused by the sudden sea-level rise at ca.  
603 6.8 ± 0.2 ka BP due to the disappearance of the west section of the Laurentide ice  
604 sheet (Blanchon and Shaw, 1995; Carlson et al., 2007). From ca. 6500 to 5600 cal. yr  
605 BP, sea water retreated slowly again and the sedimentary environment transitioned  
606 gradually from salt marsh to freshwater marsh in the area near core DTX4, reflected  
607 by the composition of organic matter over this period (Fig. 5), while site DTX10 was  
608 subaerially exposed (1.0-0.88 m in Fig. 7). Correspondingly, the infilling rate of the  
609 Palaeo-Taihu Estuary fell dramatically, likely signifying a process of shrinking due to  
610 the stable or slightly declining sea level from ~6300 cal. yr BP (Fairbanks, 1989; Bard  
611 et al., 1996; Bird et al., 2007; Wang et al., accepted). After ca. 5600 cal. yr BP, the  
612 East Tiaoxi River Plain transitioned through a range of environments from stable  
613 freshwater marsh (core DTX4) or dry land (core DTX10), characterised by freshwater  
614 benthic diatoms and C<sub>3</sub> terrestrial plants respectively (Fig. 3-7). In other words, no sea  
615 water penetration occurred and entirely freshwater environments persisted from ca.  
616 5600 cal. yr BP throughout to the present. In terms of the Palaeo-Taihu Estuary, it  
617 likely shrank dramatically as it was filled up with sediment.

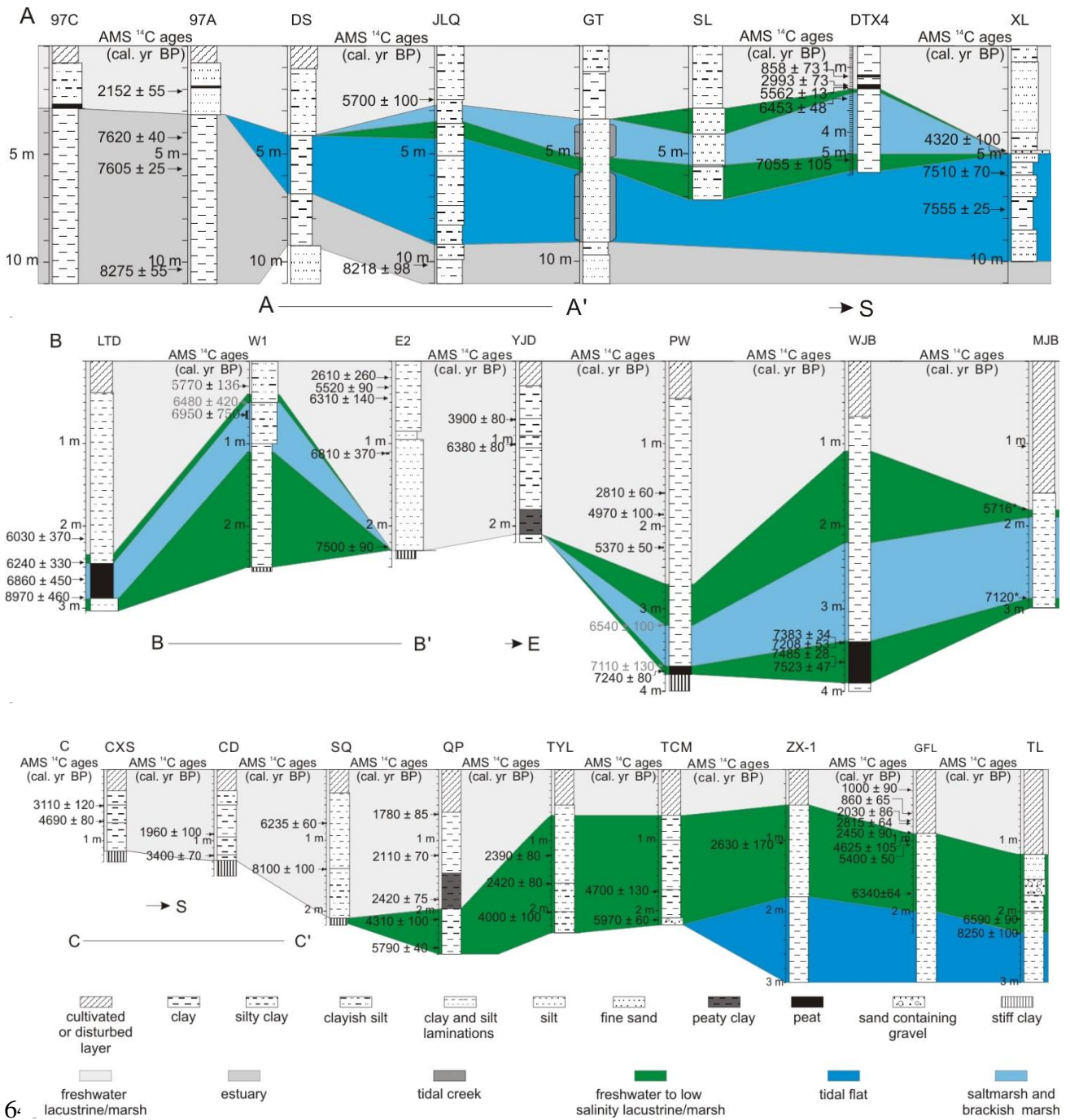
618 This study also demonstrates that viable and informative diatom counts can be  
619 made using the sodium polytungstate (SPT) density separation technique even on  
620 material which has very low diatom concentrations (here, largely as a result of  
621 dissolution). There is some indication that there is some preferential recovery of  
622 certain taxa (compare adjacent samples using the standard water-bath and SPT  
623 method in core DTX10 in Figure 4, for example for *Diploneis smithii* in Zone I) but  
624 there is clearly little systematic difference between the two methods, thus confirming

625 the utility of the approach in such sediments. Results here support the use of SPT as a  
626 very useful technique which may have wider application in estuarine and marine  
627 sediments, where the option of working on material with well-preserved or abundant  
628 diatoms (or other siliceous remains) may simply not be available, and yet may deliver  
629 much information of great palaeoecological value, even with poorly preserved  
630 assemblages (cf. [Ryves et al. 2006, 2009](#)).

### 631 *5.2 Environmental changes in the whole Taihu Plain*

632 We recognise six stages for the morphological and hydrologic evolution of the  
633 Palaeo-Taihu Estuary according to the multi-proxy analyses in cores DTX4 and  
634 DTX10. Before 7500 cal. yr BP, it was a high salinity estuary; 7500-7100 cal. yr BP, a  
635 low salinity estuary influenced strongly by the Yangtze freshwater discharge;  
636 7100-7000 cal. yr BP, it developed into a low salinity to freshwater marsh; 7000-6500  
637 cal. yr BP, salt water penetrated into the marsh; 6500-5600 cal. yr BP, gradual retreat  
638 of marine influence; and from 5600 cal. yr BP, stable freshwater conditions. A similar  
639 history of hydrologic change can be inferred from the stratigraphic transections across  
640 the Taihu Plain ([Fig. 8](#)).





644 **Fig. 8.** Stratigraphic transections of collected cores, including section A-A' (A) and  
645 B-B' (B)  
646 and C-C' (C). In section A-A', core 97C is after [Ding \(2004\)](#), core 97A after [Zhou and Zheng \(2000\)](#),  
and core DS, JLQ, GT and SL are after [Yan and Huang \(1987\)](#) and [Hong \(1991\)](#), and core XL is after

647 Liu et al. (2015). In section B-B', site LTD is after Li et al. (2008), core W1 after Chang et al. (1994)  
648 and Wang et al. (2001), core E2 after Wang et al. (2001), core YJD and PW after Zong et al. (2011,  
649 2012b) and Innes et al. (2014), core WJB after Qin et al. (2011) and MJB after Long et al. (2014). In  
650 section C-C', core CXS, CD and TYL are after Zong et al. (2012b), core SQ, TCM and TL after Zong  
651 et al. (2011), core QP after Atahan et al. (2008) and Itzstein-Davey et al. (2007), ZX-1 after Chen et al.  
652 (2005) and Tao et al. (2006) and core GEL after Wang et al. (2012). 0 m is the start depth for each core.  
653 Ages in black are from references for each core and ages in grey black are linearly interpolated based  
654 on "Clam" (Blaauw, 2010).

655 Estuarine facies dominated before 7500 cal. yr BP in multiple cores including  
656 97C, 97A, DS, JLQ, GT and XL in the palaeo-Taihu Estuary (Fig. 8A; references for  
657 these cores are in Supplementary Table 1), due to rapid sea-level rise in the early  
658 Holocene (Wang et al., 2012). The sedimentary facies then turned into tidal flat in  
659 these cores around 7500 cal. yr BP owing to the infilling of the estuary (Fig. 8A).  
660 Brackish tidal flat conditions also occurred in other cores like ZX-1, GFL and TL in  
661 the east Taihu Plain (Fig. 8C). As the relative sea level reached approximately -6 m at  
662 7500 cal. yr BP (Wang et al., 2012), the late Pleistocene interfluvial terrace T1 region  
663 (including around Shanghai City) was a shallow sea environment due to this  
664 transgressive phase (Li et al., 2001; Zong et al., 2004; Wang et al., 2012, 2013). No  
665 sea water penetration occurred throughout the Holocene in the region of the late  
666 Pleistocene interfluvial terrace T3 (Fig. 1C) where palaeo-altitude was the highest  
667 during the LGM (as recorded in core E2, YJD, CD, CXS and SQ; Fig. 8B and 8C).  
668 The central Taihu Plain was isolated from western uplands due to sea water  
669 inundation through the Palaeo-Taihu Estuary at ca. 7500 cal. yr BP (Fig. 9A).

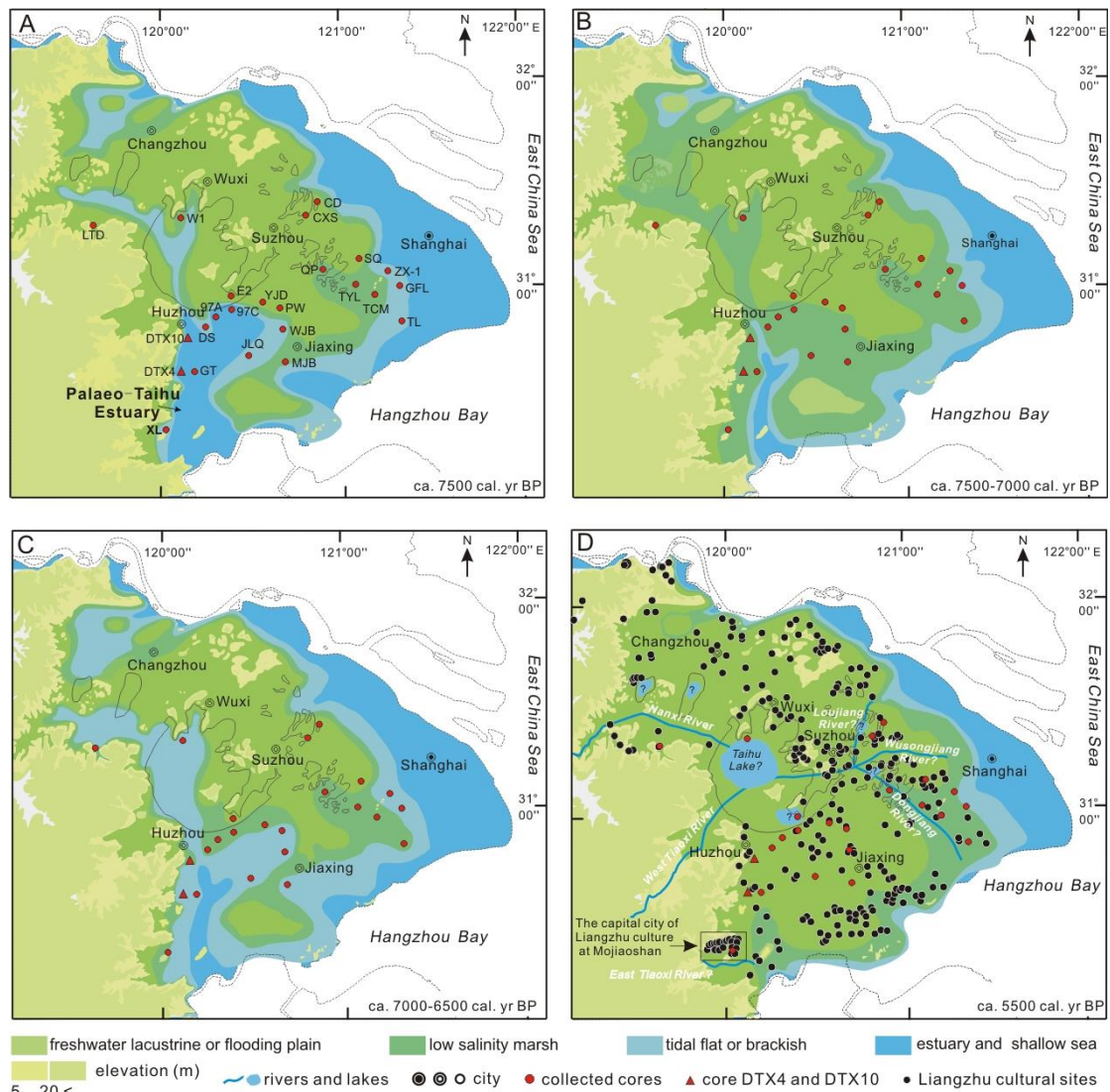


**Fig. 9.** Palaeogeographic map for the Taihu Plain before ca. 7500 cal. yr BP (A), during ca. 7500-7000 cal. yr BP (B), during ca. 7000-6500 cal. yr BP (C), and at ca. 5500 cal. yr BP (D). Rivers in (D) are based on Hong (1991), and the possible formation of Taihu Lake is based on Wang et al. (2001). The number of Liangzhu (5500-4500 cal. yr BP) cultural sites grew rapidly to 461, while it is only 78 and 93 during the Majiabang (7000-5800 cal. yr BP) and Songze (5800-5500 cal. yr BP) period, respectively (from Zheng, 2002; Chen, 2002; Xu, 2015).

678 The marine regression at ca. 7500-7000 cal. yr BP recorded in core DTX4 and  
679 DTX10 was also seen in cores in the Palaeo-Taihu Estuary (e.g. cores JLQ, GT and  
680 WJB; Fig. 8A). In the central Taihu Plain, low salinity to freshwater marshes  
681 developed at ca. 7600-7120 cal. yr BP in core WJB (Fig. 8B), indicated by reduced  
682 concentration of marine dinoflagellate cysts and *Chenopodiaceae* pollen (Qin et al.,  
683 2011). Consequently, this sea water regression event promoted the rapid expansion of  
684 low salinity to freshwater marshes, especially in the area of the Palaeo-Taihu valley  
685 (Fig. 9B).

686 Evidence for sea water penetration after 7000 cal. yr BP was found in several  
687 sediment cores (e.g. PW, WJB, MJB) in the central Taihu Plain (Fig. 8B) in addition  
688 to those in the Palaeo-Taihu Estuary (Fig. 8A). Moreover, this marine transgression  
689 reached areas where no sea water influence was observed in the records before. For  
690 example, the foraminifera *Ammonia compressiuscula* and *Ammonia* *cff.* *sobrina*,  
691 which prefer brackish tidal flat environments, occurred for the first time in the peat  
692 layer dated at ca. 7000 cal. yr BP at site LTD, located at the head of the Palaeo-Taihu  
693 valley, northwest of the Taihu Plain (Li et al., 2008; Fig. 8B). Marine and brackish  
694 diatom species, marine species of dinoflagellate cysts and foraminifera were only  
695 found at 50-90 cm (dated at ca. 7000 cal. yr BP) in core W1 in the north part of Taihu  
696 Lake (Fig. 8B and 9C; Chang et al., 1994, Wang et al., 2001). Sea water also  
697 inundated the low salinity marsh around core PW in the south east Taihu Plain at  
698 some time after 7200 cal. yr BP (Fig. 8B; Zong et al., 2011; Innes et al., 2014).  
699 Therefore, the transgression between ca. 7000-6500 cal. yr BP influenced a large area,  
700 including the innermost Taihu Plain, through low-lying area such as the Palaeo-Taihu  
701 valley (Fig. 9C). Low salinity marsh then returned from ca. 6200 to 5600 cal. yr BP at  
702 sites LTD, W1, PW and DTX4 (Fig. 8), and thereafter stable freshwater conditions in

703 the central Taihu Plain developed completely after ca. 5600 cal. yr BP, likely  
704 indicating the closure of the Palaeo-Taihu Estuary (Fig. 9D).

### 705 *5.3 Role of hydrological environments on the development of rice farming*

706 Rice growth is susceptible to salinity conditions and demands suitable water  
707 depth, in addition to warm and humid climate (Zeng et al., 2003; Yu et al., 2000; Chen  
708 et al., 2005; Innes et al., 2009, 2014; Patalano et al., 2015). The Taihu Plain was  
709 semi-encircled by sea water before ca. 7500 cal. yr BP (Fig. 9A), corresponding with  
710 no sedentary Neolithic settlements and no remains of rice cultivation (Mo et al., 2011).  
711 Concurrent with withdrawal of sea water and expansion of low salinity and freshwater  
712 marshes between ca. 7500 cal. yr BP and ca. 7000 cal. yr BP, rice cultivation began  
713 (Cao et al., 2006; Fuller et al., 2007; Mo et al., 2011; Zong et al., 2011) and the  
714 Majiabang culture developed in the Taihu Plain, in addition to benefits of heat and  
715 precipitation provided by the optimum climate (Chen et al., 2005; Wang et al., 2005).  
716 However, no rapid advance in rice cultivation or productivity, or in the number of  
717 Neolithic sites, occurred during the late Majiabang and early Songze period. This is  
718 likely due to the lack of adequate freshwater supply, because the central Taihu plain  
719 was isolated from the western uplands by the Taihu-Palaeo Estuary until at around  
720 5600 cal. yr BP (Fig. 9), and hence no river discharge from the western uplands  
721 entered the central Taihu plain.

722 We further suggest that the freshening of the East Tiaoxi River Plain or the  
723 shrinkage/closure of the Palaeo-Taihu Estuary at ca. 5600 cal. yr BP, was critical for  
724 the rapid expansion of rice agriculture across the whole Taihu Plain during the  
725 Liangzhu period (Fig. 9D), in the context of deteriorating climate conditions  
726 compared with the Majiabang and Songze period (Wang et al., 2005; Innes et al.,  
727 2014). Firstly, the shrinkage/closure of the Palaeo-Taihu Estuary, which is supported

728 by extensive distribution of Liangzhu cultural sites in the Tiaoxi River Plain (Zheng,  
729 2002), prevented the intrusion of sea water from Hangzhou Bay into the Taihu Plain,  
730 allowing freshwater conditions, particularly in the southern and western parts.  
731 Secondly, it restricted the discharge of freshwater from the western uplands (e.g. the  
732 west Tiaoxi river) into the Hangzhou Bay, and instead, forced this freshwater to flow  
733 eastwards, likely forming three previously existing rivers: the Loujiang River, the  
734 Wusongjiang River and the Dongjiang River (Fig. 9D; Hong, 1991). This increasing  
735 density of the river network would provide an increasing area of freshwater wetlands  
736 available to be transformed into rice paddies and greater quantity of fresh water for  
737 the east Taihu Plain. This conjecture is supported by the fact that the area of rice  
738 paddy fields excavated in several archeological sites recently was several times larger  
739 during the Liangzhu period than during the Majiabang and Songze period, and were  
740 connected to natural and artificial creeks, instead of wells and ponds, which had  
741 stronger capability of water storage (Cao et al., 2007; Hu et al., 2013; Zheng et al.,  
742 2014; Zhuang et al., 2014). Thirdly, new or enlarged freshwater marsh environments  
743 of the East Tiaoxi River Plain would have supplied additional freshwater wetland  
744 resources. Lastly, water level rise, in response to sea-level rise after the Taihu Plain  
745 was separated from the Hangzhou Bay and the East China Sea, would also encourage  
746 formation of freshwater wetlands (Hong, 1991; Chen et al., 1997). All these  
747 advantages together would have increased opportunity for domesticated rice  
748 cultivation in the whole Taihu Plain and rice productivity, supporting the continuous  
749 and dramatic advancement of the Liangzhu culture.

750 We also speculate that the terrestrialisation and freshening of the East Tiaoxi  
751 River Plain may have facilitated communication between the north and east Taihu  
752 Plain, with the capital city of Liangzhu at Mojiaoshan, southwest of Taihu Plain (Fig.  
753 9D) and even with areas south of Hangzhou Bay (Chen, 2015; Xu, 2015), given the

754 barrier that the Palaeo-Taihu Estuary would have represented. Such easier  
755 communication would support the development and flourishing of the Liangzhu  
756 capital city. In return, the capital city would be act as a hub for advanced technology  
757 and cultural innovation, promoting the further expansion of rice farming and cultural  
758 development in the region over the Liangzhu period.

759

## 760 **6. Conclusions**

761 A multiproxy sedimentological analysis combining chronological, lithological,  
762 geochemical and biological analyses of two sediment cores (DTX4 and DTX10)  
763 collected from the East Tiaoxi River Plain, southern Yangtze delta Plain, have shed  
764 light on changes in landscape and hydrology in this region over the last 7500 years.  
765 Before ca. 7500 cal. yr BP, the Palaeo-Taihu Estuary existed along the present day  
766 East Tiaoxi River Plain. It infilled rapidly by ca. 7500 cal. yr BP and was  
767 characterised by low salinity conditions, because of the large supply of freshwater  
768 from the Yangtze. Sea water, however, again penetrated the East Tiaoxi River Plain  
769 after ca. 7000 cal. yr BP due to an abrupt sea-level rise, and a salt marsh environment  
770 developed. This transgression was also recorded in other parts of the Taihu Plain  
771 where no sea water influence occurred before, hence, it was possibly the largest  
772 sea-level transgression during the Holocene, based on the synthesis of a large number  
773 of hydrological and environmental records from the region. After ca. 6500 cal. yr BP,  
774 sea-water penetration gradually declined and infilling rate of the Palaeo-Taihu Estuary  
775 fell owing to slowing sea-level rise. The dramatic shrinkage/closure of the  
776 Palaeo-Taihu Estuary occurred after ca. 5600 cal. yr BP, corresponding to the  
777 formation of stable freshwater marsh (or subaerial land) conditions in the East Tiaoxi  
778 River Plain.

779 Geomorphological and hydrological changes in the East Tiaoxi River Plain  
780 played an important role in the rise of rice cultivation and development of Neolithic  
781 cultures across the Taihu Plain. Especially, the freshening of the East Tiaoxi River  
782 Plain or its terrestrialisation after ca. 5600 cal. yr BP, was likely one critical  
783 precondition encouraging rapid increase of rice productivity (and so cultural  
784 development) during the Liangzhu period.

785

## 786 **Acknowledgments**

787 This study was supported by the National Natural Science Foundation of China  
788 (Grant No. 41576042) and the China Scholarship Council Postgraduate Scholarship  
789 Program, which allowed TC spending a year at Loughborough University. We are  
790 grateful to two anonymous reviewers for their helpful comments.

791

792

## 793 **References**

794 Atahan, P., Itzstein-Davey, F., Taylor, D., Dodson, J., Qin, J., Zheng, H., Brooks,  
795 A., 2008. [Holocene-aged sedimentary records of environmental changes and early  
796 agriculture in the lower Yangtze, China. Quaternary Science Reviews 27, 556-570.](#)

797 Bard, E., Hamelin, B., Arnold, M., Montaggioni, L., Cabioch, G., Faure, G.,  
798 Rougerie, F., 1996. [Deglacial sea-level record from Tahiti corals and the timing of  
799 global meltwater discharge. Nature 382, 241-244.](#)

800 Battarbee, R.W., Jones, V.J., Flower, R.J., Cameron, N.G., Bennion, H.,  
801 Carvalho, L., Juggins, S., 2001. [Diatoms, in: Smol, J.P., Birks, H.J.B., Last, W.M.,](#)



802 Bradley, R.S., Alverson, K. (Eds.), Tracking Environmental Change Using Lake  
803 Sediments: Terrestrial, Algal, and Siliceous Indicators. Springer Netherlands,  
804 Dordrecht, pp. 155-202.

805 Battarbee, R.W., Kneen, M.J., 1982. The use of electronically counted  
806 microsphere sin absolute diatom analysis. *Limnology & Oceanography* 27, 184-188.

807 Beuselinck, L., Govers, G., Poesen, J., Degraer, G., Froyen, L., 1998. Grain-size  
808 analysis by laser diffractometry: comparison with the sieve-pipette method. *Catena* 32,  
809 193-208.

810 Bird, M., Fifield, L., Teh, T., Chang, C., Shirlaw, N., Lambeck, K., 2007. An  
811 inflection in the rate of early mid-Holocene eustatic sea-level rise: A new sea-level  
812 curve from Singapore. *Estuarine, Coastal and Shelf Science* 71, 523-536.

813 Blaauw, M., 2010. Methods and code for ‘classical’ age-modelling of  
814 radiocarbon sequences. *Quaternary Geochronology* 5, 512-518.

815 Blanchon, P., Shaw, J., 1995. Reef drowning during the last deglaciation:  
816 Evidence for catastrophic sea-level rise and ice-sheet collapse. *Geology* 23, 4-8.

817 Cao, Z.H., Ding, J.L., Hu, Z.Y., Knicker, H., Kögel-Knabner, I., Yang, L.Z., Yin,  
818 R., Lin, X.G., Dong, Y.H., 2006. Ancient paddy soils from the Neolithic age in  
819 China’s Yangtze River Delta. *Naturwissenschaften* 93, 232-236.

820 Cao, Z.H., Yang, L.Z., Lin, X.G., Hu, Z.Y., Dong, Y. H., Zhang, G.Y., Lu, Y.C.,  
821 Yin, R., Wu, Y.L., Ding, J.L., Zheng, Y.F., 2007. Morphological characteristics of  
822 paddy fields, paddy soil profile, phytolith and fossil rice grain of the Neolithic age in  
823 Yangtze river delta. *Acta Pedologica Sinica* 44, 838-847 (In Chinese, with English  
824 abstract).

825 Carlson, A.E., Clark, P.U., Raisbeck, G.M., Brook, E.J., 2007. Rapid Holocene  
826 Deglaciation of the Labrador Sector of the Laurentide Ice Sheet. *Journal of Climate*  
827 20, 5126-5133.

828 Chang, W.Y.B., Xu, X.M., Yang, J.R., Liu, J.L., 1994. Evolution in Taihu Lake  
829 ecosystem as evidence of changes in sediment profiles. *Journal of Lake Science* 6,  
830 217-226.

831 Chappell, J., Polach, H., 1991. Post-glacial sea-level rise from a coral record at  
832 Huon Peninsula, Papua New Guinea. *Nature* 349, 147-149.

833 Chen, J., 2002. Neolithic cultures in the Yangtze delta, China and their  
834 environments. PhD Thesis, East China Normal University, China (in Chinese, with  
835 English abstract).

836 Chen, J., 2015. The Formation of the Songze Culture. *Relics from South* 1, 57-65  
837 (in Chinese, with English abstract).

838 Chen, X., Yang, X., Dong, X., Liu, Q., 2011. Nutrient dynamics linked to  
839 hydrological condition and anthropogenic nutrient loading in Chaohu Lake (southeast  
840 China). *Hydrobiologia* 661, 223-234.

841 Chen, Z., Hong, X., Li, S., Wang, L., Shi, X., 1997. Study of archaeology-related  
842 environment evolution of Taihu Lake in southern Chang Jiang Delta Plain. *Acta*  
843 *Geographica Sinica* 52, 131-137 (in Chinese, with English abstract).

844 Chen, Z., Wang, Z., Schneiderman, J., Taol, J., Cail, Y., 2005. Holocene climate  
845 fluctuations in the Yangtze delta of eastern China and the Neolithic response. *The*  
846 *Holocene* 15, 915-924.

847           Chen, Z.Y., Zong, Y.Q., Wang, Z.H., Wang, H., Chen, J., 2008. Migration  
848 patterns of Neolithic settlements on the abandoned Yellow and Yangtze River deltas  
849 of China. *Quaternary Research* 70, 301-314.

850           Ding, Y. F., 2004. Deposit record of climate and environmental changes of Taihu  
851 Lake since 10,000 a. Master Thesis, East China Normal University, China (in Chinese,  
852 with English abstract).

853           Dong, X., Bennion, H., Battarbee, R., Yang, X., Yang, H., Liu, E., 2008.  
854 Tracking eutrophication in Taihu Lake using the diatom record: potential and  
855 problems. *Journal of Paleolimnology* 40, 413-429.

856           Fairbanks, R.G., 1989. A 17, 000-year glacio-eustatic sea level record: influence  
857 of glacial melting rates on the Younger Dryas event and deep-ocean circulation.  
858 *Nature* 342, 637-642.

859           Fan, Y. P., 2011. On the development of rice farming in Tailake area during the  
860 Neolithic age of China. Master Thesis, Nanjing Agriculture University, China (in  
861 Chinese, with English abstract).

862           Fuller, D.Q., Harvey, E., LING, Q., 2007. Presumed domestication? Evidence  
863 for wild rice cultivation and domestication in the fifth millennium BC of the Lower  
864 Yangtze region. *Antiquity* 81, 316-331.

865           Gell, P., Tibby, J., Little, F., Baldwin, D., Hancock, G., 2007. The impact of  
866 regulation and salinisation on floodplain lakes: The lower River Murray, Australia.  
867 *Hydrobiologia* 591, 135-146.

868           Grönlund, T., 1993. Diatoms in surface sediments of the Gotland Basin in the  
869 Baltic Sea. *Hydrobiologia* 269-270, 235-242.

870 Hasle, G.R., Syvertsen, E.E., 1996. Chapter 2-Marine Diatoms. Identifying  
871 Marine Diatoms & Dinoflagellates, 5-385.

872 Hong, X., 1991. Origin and evolution of the Taihu Lake. Marine Geology and  
873 Quaternary Geology 11, 87-99 (in Chinese, with English abstract).

874 Hu, L., Chao, Z., Gu, M., Li, F., Chen, L., Liu, B., Li, X., Huang, Z., Li, Y.,  
875 Xing, B., 2013. Evidence for a Neolithic Age fire-irrigation paddy cultivation system  
876 in the lower Yangtze River Delta, China. Journal of Archaeological Science 40,  
877 72-78.

878 Innes, J.B., Zong, Y., Chen, Z., Chen, C., Wang, Z., Wang, H., 2009.  
879 Environmental history, palaeoecology and human activity at the early Neolithic  
880 forager/cultivator site at Kuahuqiao, Hangzhou, eastern China. Quaternary Science  
881 Reviews 28, 2277-2294.

882 Innes, J.B., Zong, Y., Wang, Z., Chen, Z., 2014. Climatic and palaeoecological  
883 changes during the mid-to Late Holocene transition in eastern China: high-resolution  
884 pollen and non-pollen palynomorph analysis at Pingwang, Yangtze coastal lowlands.  
885 Quaternary Science Reviews 99, 164-175.

886 Itzstein-Davey, F., Atahan, P., Dodson, J., Taylor, D., Zheng, H., 2007.  
887 Environmental and cultural changes during the terminal Neolithic: Qingpu, Yangtze  
888 delta, eastern China. The Holocene 17, 875-887.

889 Jiang, L., Liu, L., 2006. New evidence for the origins of sedentism and rice  
890 domestication in the Lower Yangzi River, China. Antiquity 80, 355-361.

891 Juggins, S., 1991-2009. C2 Data Analysis. Newcastle University, Newcastle.  
892 Available at: <http://www.staff.ncl.ac.uk/staff/stephen.juggins/software/C2Home.htm>.

893 Juggins, S., 2013. Quantitative reconstructions in palaeolimnology: new  
894 paradigm or sick science? *Quaternary Science Reviews* 64, 20-32.

895 Kilham, P., 1990. Ecology of *Melosira* Species in the Great Lakes of Africa, in:  
896 Tilzer, M.M., Serruya, C. (Eds.), *Large Lakes: Ecological Structure and Function*.  
897 Springer Berlin Heidelberg, Berlin, Heidelberg, pp. 414-427.

898 Krammer, K., Lange-Bertalot, H., 1986. Bacillariophyceae. 1: Teil: Naviculaceae.  
899 In: Ettl, H., Gärtner, G., Gerloff, J., Heynig, H., Mollenhauer, D. (Eds.),  
900 Süßwasserflora von Mitteleuropa, Band 2/1. Gustav Fischer Verlag, Stuttgart, New  
901 York.

902 Krammer, K., Lange-Bertalot, H., 1988. Bacillariophyceae. 2: Teil:  
903 Bacillariaceae, Epithemiaceae, Surirellaceae. In: Ettl, H., Gärtner, G., Gerloff, J.,  
904 Heynig, H., Mollenhauer, D. (Eds.), Süßwasserflora von Mitteleuropa, Band 2/2.  
905 Gustav Fischer Verlag, Stuttgart, New York.

906 Krammer, K., Lange-Bertalot, H., 1991a. Bacillariophyceae. 3: Teil: Centrales,  
907 Fragilariaceae, Eunotiaceae. In: Ettl, H., Gärtner, G., Gerloff, J., Heynig, H.,  
908 Mollenhauer, D. (Eds.), Süßwasserflora von Mitteleuropa, Band 2/3. Gustav Fischer  
909 Verlag, Stuttgart, Jena.

910 Krammer, K., Lange-Bertalot, H., 1991b. Bacillariophyceae. 4: Teil:  
911 achnanthaceae. In: Ettl, H., Gärtner, G., Gerloff, J., Heynig, H., Mollenhauer, D.  
912 (Eds.), Süßwasserflora von Mitteleuropa, Band 2/4. Gustav Fischer Verlag, Stuttgart,  
913 Jena.

914 Lamb, A.L., Vane, C.H., Wilson, G.P., Rees, J.G., Moss-Hayes, V.L., 2007.  
915 Assessing  $\delta^{13}\text{C}$  and C/N ratios from organic material in archived cores as Holocene

916 sea level and palaeoenvironmental indicators in the Humber Estuary, UK. *Marine*  
917 *geology* 244, 109-128.

918 Lawler, A., 2009. *Beyond the Yellow River: How China Became China*. *Science*  
919 325, 930-935.

920 Leng, M.J., Lewis, J.P., 2017. C/N ratios and Carbon Isotope Composition of  
921 Organic Matter in Estuarine Environments, in: Weckström, K., Saunders, K.M., Gell,  
922 P.A., Skilbeck, C.G. (Eds.), *Applications of Palaeoenvironmental Techniques in*  
923 *Estuarine Studies*. Springer Netherlands, Dordrecht, pp. 213-237.

924 Li, C.X., Chen, Q.Q., Zhang, J.Q., Yang, S., Fan, D., 2000. Stratigraphy and  
925 paleoenvironmental changes in the Yangtze Delta during the Late Quaternary. *Journal*  
926 *of Asian Earth Sciences* 18, 453-469.

927 Li, C.X., Wang, P.X., Sun, H.P., Zhang, J.Q., Fan, D., Deng, B., 2002. Late  
928 Quaternary incised-valley fill of the Yangtze delta (China): its stratigraphic  
929 framework and evolution. *Sedimentary Geology* 152, 133-158.

930 Li, L., Zhu, C., Lin, L., Zhao, Q., Shi, G., Zhu, H., 2008. Transgression records  
931 between 7500-5400 BC on the stratum of the Luotuodun site in Yixing, Jiangsu  
932 province. *Acta Geographica Sinica* 63, 1189-1197.

933 Liu, L., Chen, X., 2012. *The archaeology of China: From the late paleolithic to*  
934 *the early bronze age*. Cambridge World Archaeology, Cambridge.

935 Liu, Q., Yang, X., Anderson, N.J., Liu, E., Dong, X., 2012. Diatom ecological  
936 response to altered hydrological forcing of a shallow lake on the Yangtze floodplain,  
937 SE China. *Ecohydrology* 5, 316-325.

938       Liu, Y., Sun, Q., Thomas, I., Zhang, L., Finlayson, B., Zhang, W., Chen, J., Chen,  
939       Z., 2015. Middle Holocene coastal environment and the rise of the Liangzhu City  
940       complex on the Yangtze delta, China. *Quaternary Research* 84, 326-334.

941       Long, T., Qin, J., Atahan, P., Mooney, S., Taylor, D., 2014. Rising waters: New  
942       geoarchaeological evidence of inundation and early agriculture from former  
943       settlement sites on the southern Yangtze Delta, China. *Holocene* 24, 546-558.

944       Meyers, P.A., 2003. Applications of organic geochemistry to paleolimnological  
945       reconstructions: a summary of examples from the Laurentian Great Lakes. *Organic*  
946       *Geochemistry* 34, 261-289.

947       Middelburg, J.J., Nieuwenhuize, J., 1998. Carbon and nitrogen stable isotopes in  
948       suspended matter and sediments from the Schelde Estuary. *Marine chemistry* 60,  
949       217-225.

950       Mo, D., Zhao, Z., Xu, J., Li, M., 2011. Holocene Environmental Changes and the  
951       Evolution of the Neolithic Cultures in China, in: Martini, P.I., Chesworth, W. (Eds.),  
952       *Landscapes and Societies: Selected Cases*. Springer Netherlands, Dordrecht, pp,  
953       299-319.

954       Müller, A., Mathesius, U., 1999. The palaeoenvironments of coastal lagoons in  
955       the southern Baltic Sea, I. The application of sedimentary C<sub>org</sub>/N ratios as source  
956       indicators of organic matter. *Palaeogeography, Palaeoclimatology, Palaeoecology* 145,  
957       1-16.

958       Müller, A., Voss, M., 1999. The palaeoenvironments of coastal lagoons in the  
959       southern Baltic Sea, II.  $\delta^{13}\text{C}$  and  $\delta^{15}\text{N}$  ratios of organic matter—sources and sediments.  
960       *Palaeogeography, Palaeoclimatology, Palaeoecology* 145, 17-32.

961 Owen, R.B., Crossley, R., 1992. Spatial and temporal distribution of diatoms in  
962 sediments of Lake Malawi, Central Africa, and ecological implications. *Journal of*  
963 *Paleolimnology* 7, 55-71.

964 Patalano, R., Wang, Z., Leng, Q., Liu, W., Zheng, Y., Sun, G., Yang, H., 2015.  
965 Hydrological changes facilitated early rice farming in the lower Yangtze River Valley  
966 in China: A molecular isotope analysis. *Geology* 43.

967 Qin, J., Taylor, D., Atahan, P., Zhang, X., Wu, G., Dodson, J., Zheng, H.,  
968 Itzstein-Davey, F., 2011. Neolithic agriculture, freshwater resources and rapid  
969 environmental changes on the lower Yangtze, China. *Quaternary Research* 75, 55-65.

970 Reimer, P.J., Baillie, M.G.L., Bard, E., Bayliss, A., Beck, J.W., Blackwell, P.G.,  
971 Ramsey, C.B., Buck, C.E., Burr, G.S., Edwards, R.L., 2009. *IntCal09 and Marine09*  
972 *Radiocarbon Age Calibration Curves, 0-50,000 Years cal. BP.* *Radiocarbon* 51,  
973 1111-1150.

974 Renberg, I., 1990. A procedure for preparing large sets of diatom slides from  
975 sediment cores. *Journal of Paleolimnology* 4, 87-90.

976 Ryu, E., Yi, S., Lee, S.-J., 2005. Late Pleistocene-Holocene paleoenvironmental  
977 changes inferred from the diatom record of the Ulleung Basin, East Sea (Sea of Japan).  
978 *Marine Micropaleontology* 55, 157-182.

979 Ryves, D.B., Juggins, S., Fritz, S.C., Battarbee, R.W., 2001. Experimental  
980 diatom dissolution and the quantification of microfossil preservation in sediments.  
981 *Palaeogeography Palaeoclimatology Palaeoecology* 172, 99-113.

982 Ryves, D.B., Clarke, A.L., Appleby, P.G., Amsinck, S.L., Jeppesen, E.,  
983 Landkildehus, F., Anderson, N.J., 2004. Reconstructing the salinity and environment



984 of the Limfjord and Vejler. *Canadian Journal of Fisheries & Aquatic Sciences* 61,  
985 1988-2006 (1919).

986 Ryves, D.B., Battarbee, R.W., Juggins, S., Fritz, S.C., Anderson, N.J., 2006.  
987 Physical and chemical predictors of diatom dissolution in freshwater and saline lake  
988 sediments in North America and West Greenland. *Limnology and Oceanography* 51,  
989 1355-1368.

990 Ryves, D.B., Battarbee, R.W., Fritz, S.C., 2009. The dilemma of disappearing  
991 diatoms: Incorporating diatom dissolution data into palaeoenvironmental modelling  
992 and reconstruction. *Quaternary Science Reviews* 28, 120-136.

993 Song, B., Li, Z., Saito, Y., Okuno, J.I., Li, Z., Lu, A., Hua, D., Li, J., Li, Y.,  
994 Nakashima, R., 2013. Initiation of the Changjiang (Yangtze) delta and its response to  
995 the mid-Holocene sea level change. *Palaeogeography Palaeoclimatology*  
996 *Palaeoecology* 388, 81-97.

997 Stabell, B., 1985. The development and succession of taxa within the diatom  
998 genus *Fragilaria* Lyngbye as a response to basin isolation from the sea. *Boreas* 14,  
999 273-286.

1000 Stanley, D.J., 2000. Radiocarbon Dates in China's Holocene Yangtze Delta:  
1001 Record of Sediment Storage and Reworking, Not Timing of Deposition. *Journal of*  
1002 *Coastal Research* 16, 1126-1132.

1003 Tada, R., Irino, T., Koizumi, I., 1999. Land-ocean linkages over orbital and  
1004 millennial timescales recorded in Late Quaternary sediments of the Japan Sea.  
1005 *Paleoceanography* 14, 236-247.

- 1006 Talma, A.S., Vogel, J.C., 1993. A Simplified Approach to Calibrating C14 Dates.  
1007 *Radiocarbon* 35 317-322.
- 1008 Tao, J., Chen, M.T., Xu, S., 2006. A Holocene environmental record from the  
1009 southern Yangtze River delta, eastern China. *Palaeogeography, Palaeoclimatology,*  
1010 *Palaeoecology* 230, 204-229.
- 1011 Thornton, S.F., McManus, J., 1994. Application of Organic Carbon and Nitrogen  
1012 Stable Isotope and C/N Ratios as Source Indicators of Organic Matter Provenance in  
1013 Estuarine Systems: Evidence from the Tay Estuary, Scotland. *Estuarine Coastal &*  
1014 *Shelf Science* 38, 219-233.
- 1015 van der Werff, A., Huls, H., 1957-1974, Reprinted 1976. *Diatomeënfloora van*  
1016 *Nederland*. Koeltz Science Publishers, Koenigstein.
- 1017 Voß, M., Struck, U., 1997. Stable nitrogen and carbon isotopes as indicator of  
1018 eutrophication of the Oder river (Baltic sea). *Marine chemistry* 59, 35-49.
- 1019 Vos, P.C., de Wolf, H., 1993. Diatoms as a tool for reconstructing sedimentary  
1020 environments in coastal wetlands; methodological aspects. *Hydrobiologia* 269,  
1021 285-296.
- 1022 Wang, C., Li, X., Lai, Z., Tan, X., Pang, S., Yang, W., 2009. Seasonal variations  
1023 of *Aulacoseira granulata* population abundance in the Pearl River Estuary. *Estuarine*  
1024 *Coastal & Shelf Science* 85, 585-592.
- 1025 Wang, J., Chen, X., Zhu, X.H., Liu, J.L., Chang, W.Y.B., 2001. Taihu Lake,  
1026 lower Yangtze drainage basin: evolution, sedimentation rate and the sea level.  
1027 *Geomorphology* 41, 183-193.

1028 Wang, Y., Cheng, H., Edwards, R.L., He, Y., Kong, X., An, Z., Wu, J., Kelly,  
1029 M.J., Dykoski, C.A., Li, X., 2005. The Holocene Asian monsoon: links to solar  
1030 changes and North Atlantic climate. *Science* 308, 854-857.

1031 Wang, Z., Zhuang, C., Saito, Y., Chen, J., Zhan, Q., Wang, X., 2012. Early  
1032 mid-Holocene sea-level change and coastal environmental response on the southern  
1033 Yangtze delta plain, China: implications for the rise of Neolithic culture. *Quaternary*  
1034 *Science Reviews* 35, 51-62.

1035 Wang, Z., Zhan, Q., Long, H., Saito, Y., Gao, X., Wu, X., Li, L., Zhao, Y., 2013.  
1036 Early to mid-Holocene rapid sea-level rise and coastal response on the southern  
1037 Yangtze delta plain, China. *Journal of Quaternary Science* 28, 659-672.

1038 Wang, Z., Ryves, D.V., Lei, S., Nian, X., Lv, Y., Tang, L., Wang, L., Wang, J.,  
1039 Chen, J., (accepted). Middle Holocene marine flooding and human response in the  
1040 south Yangtze coastal plain, East China. *Quaternary Science reviews*.

1041 Wilson, G.P., Lamb, A.L., Leng, M.J., Gonzalez, S., Huddart, D., 2005.  $\delta^{13}\text{C}$  and  
1042 C/N as potential coastal palaeoenvironmental indicators in the Mersey Estuary, UK.  
1043 *Quaternary Science Reviews* 24, 2015-2029.

1044 Witkowski, A., Dr, Ichtologii, Lange-Bertalot, H., Metzeltin, D., 2000. *Diatom*  
1045 *flora of marine coasts I*. A.R.G. Gantner Verlag K.G.

1046 Xu, P., 2015. Research on the archaeological cultures of Neolithic age in  
1047 Ningzhen area and Huantaihu area. PhD Thesis, Jilin University, China (in Chinese,  
1048 with English abstract).

- 1049 Yan, Q., Huang, S., 1987. Evolution of Holocene sedimentary environment in  
1050 the Hangzhou-Jiaxing-Huzhou Plain. *Acta Geographica Sinica* 42, 1-15 (in Chinese,  
1051 with English abstract).
- 1052 Yang, S., Tang, M., Yim, W.W.S., Zong, Y., Huang, G., Switzer, A.D., Saito, Y.,  
1053 2011. Burial of organic carbon in Holocene sediments of the Zhujiang (Pearl River)  
1054 and Changjiang (Yangtze River) estuaries. *Marine chemistry* 123, 1-10.
- 1055 Yu, S., Zhu, C., Song, J., Qu, W., 2000. Role of climate in the rise and fall of  
1056 Neolithic cultures on the Yangtze Delta. *Boreas* 29, 157-165.
- 1057 Zeng, L., Lesch, S.M., Grieve, C.M., 2003. Rice growth and yield respond to  
1058 changes in water depth and salinity stress. *Agricultural Water Management* 59, 67-75.
- 1059 Zhan, Q., Wang, Z.H., Xie, Y., Xie, J., He, Z., 2012. Assessing C/N and  $\delta^{13}\text{C}$  as  
1060 indicators of Holocene sea level and freshwater discharge changes in the subaqueous  
1061 Yangtze delta, China. *The Holocene* 22, 697-704.
- 1062 Zhang, J., Wu, Y., Jennerjahn, T.C., Ittekkot, V., He, Q., 2007. Distribution of  
1063 organic matter in the Changjiang (Yangtze River) Estuary and their stable carbon and  
1064 nitrogen isotopic ratios: Implications for source discrimination and sedimentary  
1065 dynamics. *Marine chemistry* 106, 111-126.
- 1066 Zhang, X., Huang, D., Deng, H., Snape, C., Meredith, W., Zhao, Y., Du, Y.,  
1067 Chen, X., Sun, Y., 2015. Radiocarbon dating of charcoal from the Bianjiashan site in  
1068 Hangzhou: New evidence for the lower age limit of the Liangzhu Culture. *Quaternary*  
1069 *Geochronology* 30, Part A, 9-17.

- 1070 Zheng, C.G., 2002. Environmental archaeology on the Temporal-Spatial  
1071 distribution of Cultures sites in Taihu Lake area during 7 ka BP - 4 ka BP. PhD Thesis,  
1072 Nanjing University, China (in Chinese, with English abstract).
- 1073 Zheng, Y. F., Chen, X.G., Ding, P., 2014. Studies on the archaeological paddy  
1074 fields at Maoshan site in Zhejiang. *Quaternary Sciences*, 34, 85-96.
- 1075 Zheng, Y., Sun, G., Chen, X., 2012. Response of rice cultivation to fluctuating  
1076 sea level during the Mid-Holocene. *Chinese Science Bulletin* 57, 370-378.
- 1077 Zhou, H., Zheng, X., 2000. The Impact of Environmental Changes on the  
1078 Development of Prehistoric Civilization: The Decline of the Ancient Liang zhu  
1079 Culture in the Southern Plain of Yangtze River Delta. *Journal of East China Normal*  
1080 *University (Natural Science)* 4, 71-77 (in Chinese, with English abstract).
- 1081 Zhu, N., 2006. Impacts of the rice farming on cultural development in the Taihu  
1082 and Hangzhou Bay area, In: Shanghai Museum (Eds.), *Symposium on the civilization*  
1083 *course of the lower reach region of the Yangzte Rvier*. Shanghai Book/paint publishers,  
1084 Shanghai, pp, 69-88 (in Chinese).
- 1085 Zhuang, Y., Ding, P., French, C., 2014. Water management and agricultural  
1086 intensification of rice farming at the late-Neolithic site of Maoshan, Lower Yangtze  
1087 River, China. *Holocene* 24, 531-545.
- 1088 Zong, Y.Q., 2004. Mid-Holocene sea-level highstand along the southeast coast  
1089 of China. *Quaternary International* 117, 55-67.
- 1090 Zong, Y., Chen, Z., Innes, J.B., Chen, C., Wang, Z., Wang, H., 2007. Fire and  
1091 flood management of coastal swamp enabled first rice paddy cultivation in east China.  
1092 *Nature* 449, 459-462.

1093 Zong, Y.Q., Innes, J.B., Wang, Z.H., Chen, Z.Y., 2011. Mid-Holocene coastal  
1094 hydrology and salinity changes in the east Taihu area of the lower Yangtze wetlands,  
1095 China. *Quaternary Research* 76, 69-82.

1096 Zong, Y., Wang, Z., Innes, J., Chen, Z., 2012a. Holocene environmental change  
1097 and Neolithic rice agriculture in the lower Yangtze region of China: A review.  
1098 *Holocene* 22, 623-635.

1099 Zong, Y., Innes, J.B., Wang, Z., Chen, Z., 2012b. Environmental change and  
1100 Neolithic settlement movement in the lower Yangtze wetlands of China. *Holocene* 22,  
1101 659-673.

1102 Zuo, X., Lu, H., Jiang, L., Zhang, J., Yang, X., Huan, X., He, K., Wang, C., Wu,  
1103 N., 2017. Dating rice remains through phytolith carbon-14 study reveals  
1104 domestication at the beginning of the Holocene. *Proceedings of the National*  
1105 *Academy of Sciences of the United States of America* 114, 6486.

1

2 **Supplementary Table 1**

3 Dating results for collected cores from previous studies

<b>Core name</b>	<b>Location</b>	<b>Depth (m)</b>	<b>Dating material</b>	<b>Conventional age (yr BP)</b>	<b>Calibrated age (2 <math>\delta</math>, cal. yr BP)</b>	<b>Reference</b>
<b>97A</b>	/	2.1	Peat	/	2305-2000 (1 $\delta$ )	Zhou and Zheng, 2000
		4.11	Plant fragment	/	7660-75809 (1 $\delta$ )	
		5.78	Plant fragment	/	7630-7580 (1 $\delta$ )	
		10.2	Shell	/	8330-8220 (1 $\delta$ )	
		13.8	Plant fragment	/	8425-8365 (1 $\delta$ )	
<b>JLQ</b>	/	2.5	Bulk organic	4975 $\pm$ 70	5597-5797	Hong, 1991; Zong et al., 2011
		11.2	Bulk organic	7400 $\pm$ 80	8039-8372	
<b>DS, SL, GT</b>	/	/	/	/	/	Hong, 1991; Yan and Huang, 1987
<b>XL</b>	30°24'05" N, 120°01'38" E	4.87	Wood	3940 $\pm$ 40	4420-4220	Liu et al., 2015
		5.9	Seed	5700 $\pm$ 40	7580-7440	
		7.6	Plant material	6420 $\pm$ 40	7560-7530	
<b>LTD</b>	31°21' N, 121°19'42" E	2.16	Mud	5281 $\pm$ 175	6400-5660	Li et al., 2008
		2.45	Peat	5464 $\pm$ 165	6570-5910	
		2.64	Peat	6016 $\pm$ 200	7310-6410	
		2.88	Peat	8036 $\pm$ 190	9430-8510	
<b>W1</b>	/	0.3	Pollen	5020 $\pm$ 75	5638-5910	Chang et al., 1994; Wang et al., 2001
		0.60-0.70	Mud	6145 $\pm$ 370	6206-7703	

---

		1.60-1.70	Mud	8575 ± 410	8544-10593	
<b>E2</b>	/	0.2	Mud	2575 ± 110	2354-2868	Chang et al., 1994; Wang et al., 2001
		0.32	Mud	4765 ± 70	5433-5607	
		0.45	Mud	5495 ± 75	6175-6448	
		1.14-1.25	Mud	5970 ± 170	6441-7184	
		2.26	Mud	6575 ± 75	7410-7585	
<b>YJD</b>	30 °59'45" N, 120 °35'31" E	0.7-0.72	Pollen residue	3570 ± 40	3816-3977	Zong et al., 2012b
		1.0-1.02	Pollen residue	5600 ± 40	6299-6453	
<b>PW</b>	30 °57'30" N, 120 °38'25" E	1.59-1.61	Pollen residue	2700 ± 40	2750-2868	Innes et al., 2014
		1.85-1.87	Pollen residue	4430 ± 40	4871-5075	
		2.25-2.27	Pollen residue	4720 ± 40	5323-5417	
		3.75-3.77	Peat	6290 ± 50	7153-7320	
<b>WJB</b>	30 °49'04" N, 120 °36'56" E	3.5-3.52	Charcoal	6410 ± 60	7245-7434	Qin et al., 2011
		3.5-3.52	Pollen residue	6250 ± 70	6970-7315	
		3.74-3.76	Peat	6600 ± 50	7431-7569	
		3.74-3.76	Peat	6630 ± 60	7429-7590	
		6-6.02	Clay	7350 ± 60	8024-8318	

---



<b>ZX-1</b>	/	1.1	Organic-rich mud	2580 ± 60	2462-2794	Chen et al., 2005; Tao et al., 2006
		4.5	Shell	4160 ± 40	3875-4221	
		8.8	Organic-rich mud	6850 ± 80	7570-7853	
<b>CXS</b>	31 °22'44" N, 120 °47'30" E	0.5-0.52	Pollen residue	2960 ± 40	2985-3234	Zong et al., 2012b
		0.72-0.74	Pollen residue	4190 ± 40	4609-4768	
<b>CD</b>	31 °24'16" N, 120 °50'37" E	0.9-0.92	Pollen residue	2000 ± 40	1867-2060	Zong et al., 2012b
		1.2-1.22	Plant fragment	3160 ± 40	3324-3459	
<b>SQ</b>	31 °11'50" N, 121 °06'25" E	0.75-0.77	Pollen residue	5410 ± 40	6175-6296	Zong et al., 2011
		1.40-1.42	Pollen residue	7310 ± 50	8005-8204	
<b>QP</b>	31 °07'44" N, 120 °54'39" E	0.62-0.64	Pollen residue	1827 ± 35	1695-1865	Atahan et al., 2008; Itzstein-Davey et al., 2007
		1.20-1.22	Pollen residue	2152 ± 35	2038-2185	
		1.82-1.84	Pollen residue	2386 ± 35	2342-2493	
		2.10-2.12	Pollen residue	3853 ± 40	4215-4409	
		2.38-2.40	Pollen residue	5780 ± 30	6498-6656	
		2.42-2.44	Pollen residue	5600 ± 40	6299-6453	
		2.5-2.52	Pollen residue	5114 ± 35	5749-5830	
		2.58-2.60	Pollen residue	4920 ± 35	5594-5718	

<b>TYL</b>	31 °11'54" N, 121 °06'40" E	1.2-1.22	Pollen residue	2330 ± 40	2304-2469	Zong et al., 2012b
		1.6-1.62	Pollen residue	2390 ± 40	2338-2505	
		2.0-2.02	Pollen residue	3680 ± 40	3897-4096	
<b>TCM</b>	31 °01'48" N, 121 °05'30" E	1.72-1.74	Pollen residue	4140 ± 40	4567-4825	Zong et al., 2011
		2.12-2.14	Pollen residue	5230 ± 40	5912-6029	
<b>GFL</b>	31 °03'52" N, 121 °11'30" E	0.28	/	1070 ± 50	909-1088	Wang et al., 2012
		0.62-0.64	Wood	945 ± 30	794-925	
		0.70-0.72	Pollen residue	2057 ± 30	1945-2118	
		0.75	/	2710 ± 40	2752-2879	
		0.88-0.90	Charcoal	2453 ± 30	2362-2544	
		1.00	/	4110 ± 40	4521-4730	
		1.05	/	4600 ± 40	5346-5466	
<b>TL</b>	30 °53'12" N, 121 °18'42" E	1.74-1.76	Charcoal	5517 ± 55	6276-6403	Zong et al., 2011
		2.1-2.12	Pollen residue	5800 ± 40	6493-6678	
		2.3-2.32	Pollen residue	7390 ± 50	8152-8344	

4

5

6

**References**

7

Atahan, P., Itzstein-Davey, F., Taylor, D., Dodson, J., Qin, J., Zheng, H., Brooks, A., 2008.

8

[Holocene-aged sedimentary records of environmental changes and early agriculture in the lower](#)

9

[Yangtze, China. \*Quaternary Science Reviews\* 27, 556-570.](#)

10

Chang, W.Y.B., Xu, X.M., Yang, J.R., Liu, J.L., 1994. [Evolution in Taihu Lake ecosystem as](#)

11

[evidence of changes in sediment profiles. \*Journal of Lake Science\* 6, 217-226.](#)

12

Chen, Z., Wang, Z., Schneiderman, J., Taol, J., Cail, Y., 2005. [Holocene climate fluctuations in](#)

13

[the Yangtze delta of eastern China and the Neolithic response. \*The Holocene\* 15, 915-924.](#)

14 Hong, X., 1991. Origin and evolution of the Taihu Lake. *Marine Geology and Quaternary*  
15 *Geology* 11, 87-99 (in Chinese, with English abstract).

16 Innes, J.B., Zong, Y., Wang, Z., Chen, Z., 2014. Climatic and palaeoecological changes during the  
17 mid-to Late Holocene transition in eastern China: high-resolution pollen and non-pollen palynomorph  
18 analysis at Pingwang, Yangtze coastal lowlands. *Quaternary Science Reviews* 99, 164-175.

19 Itzstein-Davey, F., Atahan, P., Dodson, J., Taylor, D., Zheng, H., 2007. Environmental and  
20 cultural changes during the terminal Neolithic: Qingpu, Yangtze delta, eastern China. *The Holocene* 17,  
21 875-887.

22 Liu, Y., Sun, Q., Thomas, I., Zhang, L., Finlayson, B., Zhang, W., Chen, J., Chen, Z., 2015.  
23 Middle Holocene coastal environment and the rise of the Liangzhu City complex on the Yangtze delta,  
24 China. *Quaternary Research* 84, 326-334.

25 Li, L., Zhu, C., Lin, L., Zhao, Q., Shi, G., Zhu, H., 2008. Transgression records between 7500-  
26 5400 BC on the stratum of the Luotuodun site in Yixing, Jiangsu province. *Acta Geographica Sinica* 63,  
27 1189-1197.

28 Qin, J., Taylor, D., Atahan, P., Zhang, X., Wu, G., Dodson, J., Zheng, H., Itzstein-Davey, F., 2011.  
29 Neolithic agriculture, freshwater resources and rapid environmental changes on the lower Yangtze,  
30 China. *Quaternary Research* 75, 55-65.

31 Tao, J., Chen, M.T., Xu, S., 2006. A Holocene environmental record from the southern Yangtze  
32 River delta, eastern China. *Palaeogeography, Palaeoclimatology, Palaeoecology* 230, 204-229.

33 Yan, Q., Huang, S., 1987. Evolution of Holocene sedimentary environment in the Hangzhou-  
34 Jiaying-Huzhou Plain. *Acta Geographica Sinica* 42, 1-15 (in Chinese, with English abstract).

35 Wang, J., Chen, X., Zhu, X.H., Liu, J.L., Chang, W.Y.B., 2001. Taihu Lake, lower Yangtze  
36 drainage basin: evolution, sedimentation rate and the sea level. *Geomorphology* 41, 183-193.

37 Wang, Z., Zhuang, C., Saito, Y., Chen, J., Zhan, Q., Wang, X., 2012. Early mid-Holocene sea-  
38 level change and coastal environmental response on the southern Yangtze delta plain, China:  
39 implications for the rise of Neolithic culture. *Quaternary Science Reviews* 35, 51-62.

40 Zhou, H., Zheng, X., 2000. The Impact of Environmental Changes on the Development of  
41 Prehistoric Civilization: The Decline of the Ancient Liang zhu Culture in the Southern Plain of  
42 Yangtze River Delta. *Journal of East China Normal University (Natural Science)* 4, 71-77 (in Chinese,  
43 with English abstract).

44 Zong, Y.Q., Innes, J.B., Wang, Z.H., Chen, Z.Y., 2011. Mid-Holocene coastal hydrology and  
45 salinity changes in the east Taihu area of the lower Yangtze wetlands, China. *Quaternary Research* 76,  
46 69-82.

47 Zong, Y., Innes, J.B., Wang, Z., Chen, Z., 2012b. Environmental change and Neolithic settlement  
48 movement in the lower Yangtze wetlands of China. *Holocene* 22, 659-673.

49  
50  
51